

# Testing the Bose-Einstein Condensate dark matter model at galactic cluster scale

Tiberiu Harko<sup>1,\*</sup> Pengxiang Liang<sup>2,†</sup> Shi-Dong Liang<sup>2,‡</sup> and Gabriela Mocanu<sup>3§</sup>

<sup>1</sup> *Department of Mathematics, University College London,  
Gower Street, London, WC1E 6BT, United Kingdom*

<sup>2</sup> *State Key Laboratory of Optoelectronic Material and Technology,  
and Guangdong Province Key Laboratory of Display Material and Technology,  
School of Physics and Engineering,*

*Sun Yat-Sen University, Guangzhou 510275, People's Republic of China and*

<sup>3</sup> *Romanian Academy, Astronomical Institute,*

*Astronomical Observatory Cluj-Napoca,*

*15 Cireșilor Street, 400487 Cluj-Napoca, Romania*

(Dated: October 22, 2015)

## Abstract

The possibility that dark matter may be in the form of a Bose-Einstein Condensate (BEC) has been extensively explored at galactic scale. In particular, good fits for the galactic rotations curves have been obtained, and upper limits for the dark matter particle mass and scattering length have been estimated. In the present paper we extend the investigation of the properties of the BEC dark matter to the galactic cluster scale, involving dark matter dominated astrophysical systems formed of thousands of galaxies each. By considering that one of the major components of a galactic cluster, the intra-cluster hot gas, is described by King's  $\beta$ -model, and that both intra-cluster gas and dark matter are in hydrostatic equilibrium, bound by the same total mass profile, we derive the mass and density profiles of the BEC dark matter. In our analysis we consider several theoretical models, corresponding to isothermal hot gas and zero temperature BEC dark matter, non-isothermal gas and zero temperature dark matter, and isothermal gas and finite temperature BEC, respectively. The properties of the finite temperature BEC dark matter cluster are investigated in detail numerically. We compare our theoretical results with the observational data of 106 galactic clusters. Using a least-squares fitting, as well as the observational results for the dark matter self-interaction cross section, we obtain some upper bounds for the mass and scattering length of the dark matter particle. Our results suggest that the mass of the dark matter particle is of the order of  $\mu\text{eV}$ , while the scattering length has values in the range of  $10^{-7}$  fm.

PACS numbers: 03.75.Kk, 11.27.+d, 98.80.Cq, 04.20.-q, 04.25.D-, 95.35.+d

---

\*Electronic address: t.harko@ucl.ac.uk

†Electronic address: lpengx@mail2.sysu.edu.cn2

‡Electronic address: stslsd@mail.sysu.edu.cn

§Electronic address: gabriela.mocanu@ubbcluj.ro

## I. INTRODUCTION

Dark matter, first introduced to explain the flat rotation curves at galactic scales, and the virial mass discrepancy at the galaxy cluster level, is presently considered to be a major component of the Universe. Dark matter, assumed to be non-baryonic and non-relativistic, is detected only by its gravitational effects at the scale of galaxies and clusters of galaxies, through observations of the motion of massive test particles [1]. However, the particle nature of dark matter still remains mysterious. The most popular candidates for the dark matter particles are the WIMP's, weakly interacting massive, lying beyond the standard model of the particle physics [2]. Other possible explanations for dark matter include self-interacting fermionic dark matter [3], scalar-field dark matter [4], or modified gravitational theories [5].

In the standard  $\Lambda$ CDM ( $\Lambda$  Cold Dark Matter) cosmological scenario dark matter is assumed to be a pressureless, low temperature cold fluid, interacting only gravitationally with itself, and with the cosmic environment. However, as was shown in [6], from the dark matter's lack of deceleration in the Bullet Cluster collision, the self-interaction cross-section  $\sigma_{DM}$  of the dark matter particles with mass  $m$  can be constrained as  $\sigma_{DM}/m < 1.25 \text{ cm}^2/\text{g}$  (68% confidence limit) for long-ranged forces. Moreover, by using the Chandra and Hubble Space Telescopes observations of 72 collisions, a significant high dark matter self-interaction cross-section  $\sigma_{DM}/m < 0.47 \text{ cm}^2/\text{g}$  (95% CL) was obtained. From a theoretical point of view Self-Interacting Dark Matter (SIDM) models were introduced in [7]. An assumption which was intensively investigated is the possibility that the dark matter self-interaction is velocity dependent, with the simplest models assuming cross sections of the form  $1/v^\alpha$ , where  $v$  is the dark matter velocity, and  $\alpha$  is a constant [8]. N-body simulations of a class of self-interacting dark matter models, having a non-power-law velocity dependence of the transfer cross section, physically motivated by a Yukawa-like gauge boson interaction, were performed in [8]. More exactly, and contrary to the standard cold dark matter model case, for self-interacting dark matter there are no subhalos that are more concentrated, as compared to what is inferred from the kinematics of the Milky Way Dwarf Spheroidal Galaxies. The rate of dark matter scattering in collapsed structures throughout the history of the Universe was estimated recently in [9]. If the scattering cross-section is velocity-independent, it turns out that dark matter particle scattering occur mainly at late times in the cosmological evolution of the Universe. On the other hand, for dark matter models with a velocity-

dependent cross-section (like, for example, the Yukawa potential interactions via a massive mediator), the scattering rate has a maximum at around  $z \sim 20$ . This maximum happens in objects with mass less than  $10^4 M_\odot$ .

However, from both a fundamental theoretical point of view, and from a phenomenological perspective, *the physically best motivated self-interacting dark matter model is represented by the Bose-Einstein Condensate dark matter model.*

The idea of the Bose-Einstein Condensation was first introduced from a statistical physical point of view in the 1920s [10, 11]. The experimental realization of the Bose-Einstein Condensation in dilute alkali gases was achieved seventy years later, in 1995 [12]. A very basic and general result in quantum statistical physics is that at very low temperatures, in a dilute Bose gas, all bosonic particles condense to the same quantum ground state, forming a Bose-Einstein Condensate (BEC). From a physical point of view the realization of a BEC is signalled by sharp peaks in both coordinate and momentum space distributions. The Bose-Einstein Condensation process starts when particles become correlated quantum mechanically, that is, when their de Broglie thermal wavelength is greater than the mean particle distance. Equivalently, the condensation is initiated when the temperature  $T$  of the system is lower than the transition one,  $T_{tr}$ , given by

$$T_{tr} = \frac{2\pi\hbar^2 \rho_{tr}^{2/3}}{\zeta^{2/3}(3/2)m^{5/3}k_B}, \quad (1)$$

where  $m$  is the particle mass in the condensate,  $\rho_{tr}$  is the transition density,  $k_B$  is Boltzmann's constant, and  $\zeta$  denotes the Riemann zeta function.

Generally, and up to now, BEC was observed and studied extensively in the laboratory, on a very small scale, rather than at a large galactic/cosmological scale. However, *the possibility that bosons also condensate on cosmological or astrophysical scales cannot be rejected a priori.* Therefore, based on the present day theoretical and experimental knowledge of the Bose-Einstein condensation processes, it is reasonable to assume the presence of some forms of condensates in the cosmic environment. Due to their superfluid properties some stellar type astrophysical objects, like neutron or quark stars, may contain a significant part of their mass in the form of a Bose-Einstein Condensate. Stars made of Bose-Einstein Condensates were investigated in [13]. Condensate stars with particle masses of the order of two neutron masses, forming Cooper pairs, and with scattering length of the order of 10-20 fm may have maximum masses of the order of  $2 M_\odot$ , maximum central densities of the order of

$0.1 - 0.3 \times 10^{16} \text{ g/cm}^3$ , and minimum radii in the range of 10-20 km.

The idea that dark matter is in the form of a Bose-Einstein Condensate was considered, mostly from a phenomenological point of view, in [14]. A systematic study of the properties of the BEC dark matter was initiated in [15]. In order to study the dark matter condensate the non-relativistic Gross-Pitaevskii (GP) in the presence of a confining gravitational potential was considered as a starting point. A significant simplification of the mathematical formalism can be achieved by introducing the Madelung representation of the wave function, a standard approach in condensed matter physics. Then the GP equation can be represented in the equivalent form of a continuity equation, and of a hydrodynamic Euler type equation. From the Madelung representation of the GP equation it follows that dark matter can be described as a non-relativistic, Newtonian Bose-Einstein gravitational condensate gas, whose density and pressure are related by a barotropic equation of state. To test the validity of the BEC dark matter model at the galactic scales the Newtonian tangential velocity equation was fitted with a sample of rotation curves of low surface brightness and dwarf galaxies, respectively. A good agreement was found between the theoretical rotation curves, and the observational data [15].

The properties of BEC dark matter were further investigated in [16, 17]. In particular, in [17] it was shown that the non-singular density profiles of the Bose-Einstein condensed dark matter generally show the presence of an extended core, whose formation is explained by the strong interaction between dark matter particles. The mean value of the logarithmic inner slope of the mass density profile of dwarf galaxies was also obtained, and it was shown that the observed value of this parameter is in agreement with the theoretical estimations obtained in the framework of the BEC dark matter model. The cosmological implications of the finite temperature BEC dark matter were considered in [18].

An interesting result in the theory of the zero temperature BEC dark matter is that in the case of a condensate with quartic non-linearity, the equation of state is polytropic with index  $n = 1$  [15]. Therefore, the corresponding Lane-Emden equation, describing the gravitational properties of the condensate, can be solved exactly, and the density profile of the dark matter can be obtained in a simple form. Once the BEC dark matter density profile is known, all the physical parameters of the condensed system (mass, radius, central density) as well as the rotational speeds can be obtained, thus leading to the possibility of a full observational test of the model.

Up to now the properties of the BEC dark matter were investigated mostly on the galactic scale. However, the second important evidence for dark matter comes from the virial mass discrepancy in galaxy clusters [19]. A galaxy cluster is a giant astrophysical object formed of hundreds to thousands of galaxies, bounded together by their own gravitational interaction. They are composed of galaxies, representing around 1% of their mass, high temperature intracluster gas, representing around 9% of the cluster mass, and dark matter, representing 90% of the their mass. The total masses obtained by measuring the velocity dispersions of the galaxies exceed the total masses of all stars in the cluster by factors of order of  $\sim 200 - 400$  [20]. The measurement of the temperature of the intracluster medium represents another strong evidence for the presence of dark matter, since the determined depth of the gravitational potential of the clusters requires a supplementary mass component [20]. Hence galaxy clusters, being dark matter dominated astrophysical structures, are the ideal testing ground for the properties of dark matter.

It is the purpose of the present paper to consider the properties of the BEC dark matter at the galactic cluster scale. Thus we extend the previous investigations of the BEC dark matter properties at the galactic scale to astrophysical systems consisting of hundreds to thousands galaxies. We begin our study with a brief review of the properties of self-interacting dark matter bosonic system in BEC state. From the non-relativistic Gross-Pitaevskii equation and its Madelung representation of the wave function, we obtain the pressure of the system for both zero temperature and finite temperature BEC dark matter. We assume that the BEC dark matter systems are bound to hydrostatic equilibrium by the gravitational potential of the cluster. Meanwhile, we consider that the hot intracluster gas, with density profile described by the standard King's  $\beta$ -model, is bound to equilibrium in the same gravitational potential. Thus, the knowledge of the hot gas distribution allows us to reconstruct the density and mass distribution of the BEC dark matter in the cluster. This reconstruction is model dependent, and in the present paper we consider three distinct cases: the case of the isothermal gas in gravitational equilibrium with zero temperature BEC dark matter, non-isothermal gas in equilibrium with zero temperature BEC dark matter, and finally, the case of the isothermal gas in equilibrium with finite temperature BEC dark matter. In each of these cases the dark matter density and mass profiles are obtained, with the radius of the cluster expressed as a function of the astrophysical parameters of the cluster. The properties of the finite temperature BEC dark matter halos in galactic clusters are investigated in detail

by using numerical methods. The fitting of the model predictions via the least- $\chi^2$  fitting with the observational data for 106 clusters [21] allows the direct determination of the ratio  $\lambda = m^3/a$  only, where  $m$  is the mass of the dark matter particle, and  $a$  is the scattering length. By combining the obtained values of  $\lambda$  with the observational self interaction cross sections, we can obtain some upper limits of the mass and scattering length of the dark matter particles.

The present paper is organized as follows. In Section II we briefly review the basic physical and astrophysical properties of the BEC dark matter, and we present the relevant equations of state for both zero temperature and finite temperatures cases. The zero temperature dark matter properties are investigated in Section III for the isothermal intracluster gas case. The cluster dark matter density and mass profiles are obtained analytically, and the theoretical predictions are compared with the observations. The effects of the variation of the gas temperature on the astrophysical parameters of the zero temperature BEC dark matter are investigated in Section IV. The case of the finite temperature BEC dark matter is considered in Section V. We discuss and conclude our results in Section VI.

## II. BASIC PROPERTIES BOSE-EINSTEIN CONDENSATE DARK MATTER AT ZERO AND FINITE TEMPERATURE

In the present Section we briefly review the main properties of the Bose-Einstein Condensate dark matter at both zero and finite temperature, and we present the results which will be used in the sequel. For an in-depth discussion of the considered issues, and of the detailed derivation of the main results, we further refer the reader to the papers and books [23]-[28].

### A. The generalized Gross-Pitaevskii equation and the hydrodynamic representation

The starting point in the study of the Bose-Einstein Condensates is the Heisenberg equation of motion for the quantum field operator  $\hat{\Phi}(\vec{r}, t)$ . At arbitrary temperatures the Heisen-

berg equation, describing the dynamics of a Bose-Einstein condensate, is given by [23–26]

$$i\hbar \frac{\partial \hat{\Phi}(\vec{r}, t)}{\partial t} = \left[ -\frac{\hbar^2}{2m} \Delta + mV_{grav}(\vec{r}, t) + g' \hat{\Phi}^\dagger(\vec{r}, t) \hat{\Phi}(\vec{r}, t) \right] \hat{\Phi}(\vec{r}, t), \quad (2)$$

where  $m$  is the mass of the particle in the condensate,  $V_{grav}(\vec{r}, t)$  is the external gravitational trapping potential, and  $g' = 4\pi a\hbar^2/m$ . In the following we denote by  $a$  the  $s$ -wave scattering length. In order to obtain Eq. (2) we have assumed that the inter-particle interaction potential is represented as a zero-range pseudo-potential of strength  $g'$ . As a next step in our study we take the average of Eq. (2) with respect to a non-equilibrium, broken symmetry ensemble. Over this ensemble the quantum field operator takes a non-zero expectation value. We denote the average of the field operator  $\hat{\Phi}(\vec{r}, t)$  by  $\Psi(\vec{r}, t)$ ,  $\Psi(\vec{r}, t) = \langle \hat{\Phi}(\vec{r}, t) \rangle$ . From a physical point of view  $\Psi(\vec{r}, t)$  represents the condensate wave-function. After averaging Eq. (2) we find the exact equation of motion of  $\Psi(\vec{r}, t)$  as

$$i\hbar \frac{\partial \Psi(\vec{r}, t)}{\partial t} = \left[ -\frac{\hbar^2}{2m} \Delta + mV_{grav}(\vec{r}, t) \right] \Psi(\vec{r}, t) + g' \langle \hat{\Phi}^\dagger(\vec{r}, t) \hat{\Phi}(\vec{r}, t) \hat{\Phi}(\vec{r}, t) \rangle. \quad (3)$$

Now we introduce the non-condensate field operator  $\tilde{\psi}(\vec{r}, t)$  by means of the definition  $\hat{\Phi}(\vec{r}, t) = \Psi(\vec{r}, t) + \tilde{\psi}(\vec{r}, t)$ . Furthermore we assume that the average value of  $\tilde{\psi}(\vec{r}, t)$  is zero,  $\langle \tilde{\psi}(\vec{r}, t) \rangle = 0$ . Therefore we can separate out the condensate component of the quantum field operator, and thus we obtain the equation of motion for  $\Psi$  in the form [23–26]

$$i\hbar \frac{\partial \Psi(\vec{r}, t)}{\partial t} = \left[ -\frac{\hbar^2}{2m} \Delta + mV_{grav}(\vec{r}, t) + g\rho_c(\vec{r}, t) + 2g\tilde{\rho}(\vec{r}, t) \right] \Psi(\vec{r}, t) + g\rho_{\tilde{m}}(\vec{r}, t) \Psi^*(\vec{r}, t) + g\rho_{\tilde{\psi}^\dagger\tilde{\psi}}(\vec{r}, t), \quad (4)$$

where we have denoted  $g = 4\pi a\hbar^2/m^2$ . In Eq. (4) we have also introduced the four densities characterizing the condensate [23–26], namely, the local condensate mass density

$$\rho_c(\vec{r}, t) = mn_c(\vec{r}, t) = m |\Psi(\vec{r}, t)|^2, \quad (5)$$

the non-condensate mass density

$$\tilde{\rho}(\vec{r}, t) = m\tilde{n}(\vec{r}, t) = m \langle \tilde{\psi}^\dagger(\vec{r}, t) \tilde{\psi}(\vec{r}, t) \rangle, \quad (6)$$

the off-diagonal (anomalous) mass density

$$\rho_{\tilde{m}}(\vec{r}, t) = m\tilde{m}(\vec{r}, t) = m \langle \tilde{\psi}(\vec{r}, t) \tilde{\psi}(\vec{r}, t) \rangle, \quad (7)$$



and, finally, the three-field correlation function density

$$\rho_{\tilde{\psi}^+\tilde{\psi}\tilde{\psi}}(\vec{r}, t) = m \left\langle \tilde{\psi}^+(\vec{r}, t) \tilde{\psi}(\vec{r}, t) \tilde{\psi}(\vec{r}, t) \right\rangle, \quad (8)$$

respectively.

In the present paper we will restrict our analysis to the range of finite temperatures where the dominant thermal excitations can be approximated as non-condensed particles of high energy, with the particles evolving in a self-consistent exterior Hartree-Fock mean field, whose local energy is [23–26]

$$\bar{\varepsilon}_p(\vec{r}, t) = \frac{\vec{p}^2}{2m} + mV_{grav}(\vec{r}, t) + 2g[\rho_c(\vec{r}, t) + \tilde{\rho}(\vec{r}, t)] = \frac{\vec{p}^2}{2m} + U_{eff}(\vec{r}, t), \quad (9)$$

where  $U_{eff}(\vec{r}, t) = mV_{grav}(\vec{r}, t) + 2g[\rho_c(\vec{r}, t) + \tilde{\rho}(\vec{r}, t)]$ . Therefore, in the present analysis we neglect the Hartree-Fock type mean field effects associated to the anomalous density  $\rho_{\tilde{m}}$ , and with the three-field correlation function  $\left\langle \tilde{\psi}^+\tilde{\psi}\tilde{\psi} \right\rangle$ , respectively. From the point of view of astrophysical applications, for dark matter halos having a large number of particles this represents a very good approximation, since one can show that the contribution of the anomalous density and of the three-field correlation function to the total density is just of the order of a few percents [24].

### 1. *Equilibrium properties of finite temperature Bose-Einstein Condensates*

One of the important properties of the finite temperature Bose-Einstein Condensates is that in the thermal cloud the collision between particles determine the non-equilibrium distribution to evolve towards the standard static Bose-Einstein distribution function  $f^0(\vec{r}, \vec{p})$  [23]. This means that the particles in the thermal cloud are in thermodynamic equilibrium between themselves. With the use of a single-particle representation spectrum it follows that the equilibrium distribution of the thermal cloud can be represented as [23, 25]

$$f^0(\vec{p}, \vec{r}, t) = [e^{\beta\bar{\varepsilon}_p(\vec{r}, t) - \tilde{\mu}} - 1]^{-1}, \quad (10)$$

where  $\beta = 1/k_B T$ , and  $\tilde{\mu}$  is the chemical potential of the thermal cloud. In order to determine the chemical potential  $\tilde{\mu}$  we make the simplifying physical assumption that the condensate and all the thermal cloud components are in local diffusive equilibrium with respect to each other. Thus, the requirement of a diffusive equilibrium between the cloud and the

condensate gives the thermodynamic condition  $\mu_c = \tilde{\mu}$ , where  $\mu_c$  is the chemical potential of the condensate. Therefore it follows that the chemical potential  $\mu_c$  of the condensate also determines the static equilibrium distribution of the particles in the thermal cloud [23–26].

The equilibrium density of the thermal excitations is obtained from the equilibrium Bose - Einstein distribution by integration over the momenta. Therefore we obtain [23–26]

$$\tilde{\rho}(\vec{r}, t) = \frac{m}{(2\pi\hbar)^3} \int d^3\vec{p} f^0(\vec{p}, \vec{r}, t) = \frac{m}{\lambda_T^3} g_{3/2}[z(\vec{r}, t)], \quad (11)$$

where  $\lambda_T = \sqrt{2\pi\hbar^2\beta/m}$  is the de Broglie thermal wavelength,  $g_{3/2}(z)$  is a so-called Bose-Einstein function, and the fugacity  $z(\vec{r}, t)$  is defined as

$$z(\vec{r}, t) = e^{\beta[\tilde{\mu} - U_{eff}(\vec{r}, t)]} = e^{-\beta g\rho_c(\vec{r}, t)}. \quad (12)$$

The pressure  $\tilde{p}$  of the thermal excitations of the BEC dark matter can be computed from the standard statistical physics definition [23, 25]

$$\tilde{p}(\vec{r}, t) = \int \frac{d\vec{p}}{(2\pi\hbar)^3} \frac{p^2}{3m} f^0(\vec{p}, \vec{r}, t), \quad (13)$$

and is given by

$$\tilde{p}(\vec{r}, t) = \frac{1}{\beta\lambda_T^3} g_{5/2}[z(\vec{r}, t)]. \quad (14)$$

The Bose-Einstein functions  $g_{3/2}(e^{-x})$  and  $g_{5/2}(e^{-x})$  can be easily computed numerically by using the following series expansions [29],

$$g_{3/2}(e^{-x}) = 2.612 - 3.544\sqrt{x} + 1.460x - 0.103x^2 + 0.00424x^3 + O(x^{7/2}). \quad (15)$$

and

$$g_{5/2}(e^{-x}) = 1.341 + 2.363x^{3/2} - 2.612x - 0.730x^2 + 0.0346x^3 + O(x^{7/2}), \quad (16)$$

respectively. For  $x < 1$ , Eqs. (15) and (16) approximates the function  $g_{3/2}(e^{-x})$  and  $g_{5/2}(e^{-x})$  with an error smaller than 1%.

## 2. The hydrodynamic representation for finite temperature Bose-Einstein Condensates

The Gross-Pitaevskii equation for finite temperature condensates can be transformed into an equivalent hydrodynamic form with the help of the Madelung representation of the wave

function given by  $\Psi(t, \vec{r}) = \sqrt{\rho_c} \exp[(i/\hbar)S(\vec{r}, t)]$ . Then, by neglecting the effects of the mean field associated with the anomalous density and the three-field correlation function, respectively, it follows that Eq. (4) can be represented as a hydrodynamic type system, given by [23–25]

$$\frac{\partial \rho_c}{\partial t} + \nabla \cdot (\rho_c \vec{v}_c) = 0, \quad (17)$$

$$\frac{\partial S}{\partial t} = - \left( \mu_c + \frac{1}{2} m \vec{v}_c^2 \right), \quad (18)$$

where the local velocity of the condensate is defined as  $\vec{v}_c(\vec{r}, t) = (\hbar/m) \nabla S$ . The chemical potential of the condensate is obtained from the relation

$$\mu_c = -\frac{\hbar^2}{2m} \frac{\Delta \sqrt{\rho_c}}{\sqrt{\rho_c}} + mV_{grav}(\vec{r}, t) + g\rho_c(\vec{r}, t) + 2g\tilde{\rho}(\vec{r}, t). \quad (19)$$

Eq. (18) can be reformulated as the Euler equation of fluid dynamics for the condensate,

$$m \frac{d\vec{v}_c}{dt} = m \left[ \frac{\partial \vec{v}_c}{\partial t} + (\vec{v}_c \cdot \nabla) \vec{v}_c \right] = -\nabla \mu_c. \quad (20)$$

The gravitational potential  $V_{grav}$  satisfies the Poisson equation,

$$m\Delta V_{grav} = 4\pi G(\rho_c + \tilde{\rho}). \quad (21)$$

The equation of state of the finite temperature condensate can be obtained from the hydrodynamical representation by using the Thomas-Fermi approximation for the condensate wave function [23] - [28]. In this approximation, the kinetic energy term  $-(\hbar^2/2m)\Delta$  of the condensate particles is considered as being negligibly small. Hence for the chemical potential of the condensate we find [24]

$$\mu_c = mV_{grav}(\vec{r}, t) + g\rho_c(\vec{r}, t) + 2g\tilde{\rho}(\vec{r}, t), \quad (22)$$

Therefore in the Thomas-Fermi approximation the Euler equation Eq. (20) takes the form

$$\rho_c \frac{d\vec{v}_c}{dt} = -\frac{g}{m} \rho_c \nabla [\rho_c + 2\tilde{\rho}] - \rho_c \nabla V_{grav}. \quad (23)$$

With the use of Eq. (22), and by taking into account the explicit expression of  $\tilde{\rho}$ , it follows that the equation of motion of the Bose-Einstein condensate, given by Eq. (23), can be written as

$$\rho_c \frac{d\vec{v}_c}{dt} = -\nabla p_c - \rho_c \nabla V_{grav}, \quad (24)$$

where we have introduced the pressure  $p_c$  of the finite temperature Bose-Einstein condensate in thermal equilibrium with a gas of thermal excitations, defined as [24]

$$p_c(T, \rho_c) = \frac{g}{2m} \rho_c^2 - 2.362 \frac{g^{3/2}}{\lambda_T^3} (k_B T)^{-1/2} \rho_c^{3/2} + 1.460 \frac{g^2}{\lambda_T^3} (k_B T)^{-1} \rho_c^2 - 0.137 \frac{g^3}{\lambda_T^3} \times (k_B T)^{-2} \rho_c^3 + 0.00636 \frac{g^4}{\lambda_T^3} (k_B T)^{-3} \rho_c^4. \quad (25)$$

## B. Physical properties of the dark matter condensate particle

The simplest Bose-Einstein Condensate dark matter model can be obtained by adopting the zero-temperature approximation. This approximation gives a good description of the rotation curves of the galactic dark matter halos [15, 17]. It also allows us, by using the galactic global astrophysical parameters (mass and radius), to make an estimate of the physical properties of the dark matter particle. By assuming that  $\tilde{\rho} \equiv 0$ , the condensate is static ( $\vec{v}_c = 0$ , spherically symmetric, and by neglecting the quantum pressure term  $(\hbar^2/2m) (\Delta\sqrt{\rho_c}/\sqrt{\rho_c})$ , from Eqs. (20) and (21) it follows that the condensate dark halo density satisfies the Lane-Emden type differential equation [15]

$$\frac{1}{r^2} \frac{d}{dr} \left( r^2 \frac{d\rho_c}{dr} \right) + \frac{Gm^3}{a\hbar^2} \rho_c = 0. \quad (26)$$

From the analysis of the properties of the static Bose-Einstein condensate dark matter halos as described by the solutions of Eq. (26) it follows that the radius  $R$  of the zero temperature condensate dark matter halo is given by  $R = \pi\sqrt{\hbar^2 a/Gm^3}$  [15]. The total mass of the  $T = 0$  condensate dark matter halo  $M$  is found as  $M = 4\pi^2 (\hbar^2 a/Gm^3)^{3/2} \rho_c = 4R^3 \rho_c(0)/\pi$ , where  $\rho_c(0)$  is the central density of the galactic halo. The mean value  $\langle \rho \rangle$  of the density of the zero temperature condensate is given by the expression  $\langle \rho \rangle = 3\rho_c(0)/\pi^2$ . From the previous results it follows that the dark matter particle mass in the condensate satisfies a mass-galactic radius relation of the form [15]

$$m = \left( \frac{\pi^2 \hbar^2 a}{GR^2} \right)^{1/3} \approx 6.73 \times 10^{-2} \times [a(\text{fm})]^{1/3} [R(\text{kpc})]^{-2/3} \text{ eV}. \quad (27)$$

For  $a \approx 1$  fm and  $R \approx 10$  kpc, we obtain a simple estimate of the mass of the condensate particle as being of the order of  $m \approx 14$  meV. On the other hand, for  $a \approx 10^6$  fm, corresponding to the values of  $a$  observed in terrestrial laboratory experiments with rubidium and cesium cold gases, we have  $m \approx 1.44$  eV.

An important observational method that can be used very successfully to obtain the physical properties of dark matter is the study of the collisions between clusters of galaxies. Typical examples of such processes are the Bullet Cluster (1E 0657-56) and the Baby Bullet (MACSJ0025-12), respectively [30, 31]. These astrophysical studies provide important constraints on the physical properties of dark matter, like, for example, its interaction cross-section with normal baryonic matter, as well as the dark matter-dark matter self-interaction cross section. If from observations one can obtain the ratio  $\sigma_m = \sigma/m$  of the self-interaction cross section  $\sigma = 4\pi a^2$  and of the dark matter particle mass  $m$ , then the mass of the dark matter particle in the Bose-Einstein Condensate galactic halo can be estimated from Eq. (27) as [24]

$$m = \left( \frac{\pi^{3/2} \hbar^2 \sqrt{\sigma_m}}{2G R^2} \right)^{2/5}. \quad (28)$$

By analyzing several sets of results from X-ray, strong lensing, weak lensing, and optical observations with the complex numerical simulations of the merging of the Bullet Cluster, an upper limit (68 % confidence) for  $\sigma_m$  of the order of  $\sigma_m < 1.25 \text{ cm}^2/\text{g}$  was determined in [30]. By adopting for  $\sigma_m$  a value of  $\sigma_m = 1.25 \text{ cm}^2/\text{g}$ , the mass of the dark matter particle in the cold Bose-Einstein Condensate dark matter halo can be constrained as having an upper limit of the order

$$m < 3.1933 \times 10^{-37} \left( \frac{R}{10 \text{ kpc}} \right)^{-4/5} \times \left( \frac{\sigma_m}{1.25 \text{ cm}^2/\text{g}} \right)^{1/5} \text{ g} = 0.1791 \times \left( \frac{R}{10 \text{ kpc}} \right)^{-4/5} \times \left( \frac{\sigma_m}{1.25 \text{ cm}^2/\text{g}} \right)^{1/5} \text{ meV}. \quad (29)$$

By using the above value for the particle mass we can constrain the scattering length  $a$  as

$$a < \sqrt{\frac{\sigma_m \times m}{4\pi}} = 1.7827 \times 10^{-19} \text{ cm} = 1.7827 \times 10^{-6} \text{ fm}. \quad (30)$$

Therefore it follows that the value of the scattering length  $a$ , obtained from the astrophysical observations of the Bullet Cluster, is much smaller than the value of  $a = 10^4 - 10^6 \text{ fm}$ , which characterises cold Bose-Einstein Condensates in terrestrial laboratory experiments [12].

A stronger constraint for the self-interaction cross section of the dark matter particles  $\sigma_m$  was proposed in [31], with  $\sigma_m \in (0.00335 \text{ cm}^2/\text{g}, 0.0559 \text{ cm}^2/\text{g})$ . This cross section range gives a dark matter particle mass of the order

$$m \approx (9.516 \times 10^{-38} - 1.670 \times 10^{-37}) \left( \frac{R}{10 \text{ kpc}} \right)^{-4/5} \text{ g} = (0.053 - 0.093) \left( \frac{R}{10 \text{ kpc}} \right)^{-4/5} \text{ meV}, \quad (31)$$

while the scattering length is of the order of

$$a \approx (5.038 - 27.255) \times 10^{-21} \text{ cm} = (5.038 - 27.255) \times 10^{-8} \text{ fm}. \quad (32)$$

### III. ZERO TEMPERATURE BEC DARK MATTER IN GALACTIC CLUSTERS

A large number of astronomical and astrophysical observations have shown that galaxies tend to concentrate in larger structures, called clusters of galaxies, with total masses ranging from  $10^{13} M_{\odot}$  for groups, and up to a few  $10^{15} M_{\odot}$  for very large systems. The morphology of a galactic cluster is generally dominated by a regular, centrally peaked main massive component [21, 32]. Usually clusters are considered to be dark matter dominated astrophysical systems. Therefore their formation and evolution is largely controlled by the gravitational interaction between their mass components. The initial conditions of the cluster mass distribution are already set in the early post-inflationary Universe, and these initial conditions completely determine the mass function of the clusters [33].

In the present Section we consider the BEC dark matter properties as derived from the observed properties of the galaxy clusters. Galaxy clusters are complex astrophysical systems, consisting of hundreds to thousands of galaxies, intergalactic gas, and dark matter, all bound together by gravity. The basic hypothesis in the study of the galactic clusters is that the intergalactic hot gas particles are in hydrostatic equilibrium under the gravity of the dark matter and of the galaxies [21]. Starting from this assumption, and by adopting some realistic astrophysical models for the gas density, the astrophysical properties of the BEC dark matter distribution can be derived theoretically, thus allowing a full comparison of the model predictions with observations.

#### A. Astrophysical parameters of BEC dark matter in galactic clusters

As a first step in our study we assume that the temperature of the dark matter in the cluster is low enough so that *all bosons* condense to form a Bose-Einstein Condensate. Since the dark matter particles are bound in hydrostatic equilibrium by the overall mass distribution of the cluster, it follows that the dark matter density  $\rho_{DM}$  and pressure  $P_{DM}$

are related to the mass of the cluster  $M(r)$  by the hydrostatic equilibrium equation

$$\frac{1}{\rho_{DM}} \frac{dP_{DM}}{dr} = -\frac{GM(r)}{r^2} \quad (33)$$

The pressure of the gravitationally bounded BEC dark matter obeys a polytropic equation of state, given by [15]

$$P_{DM} = \frac{2\pi\hbar^2 a}{m^3} \rho_{DM}^2 \quad (34)$$

where  $m$  and  $a$  are the mass and the scattering length of the dark matter particles in the condensate. Eq. (34) can be derived from the hydrodynamic representation of the BECs, given by Eqs. (20) and (21). For the interstellar gas distribution we adopt King's  $\beta$ -model, in which the number density  $n_g$  of the hot gas is given by [21]

$$n_g(r) = n_g(0) \left(1 + \frac{r^2}{r_c^2}\right)^{-3\beta/2}, \quad (35)$$

where  $n_g(0)$  is the central number density of the gas,  $r_c$  is the core radius, and  $\beta$  is a constant. The gas is assumed to obey the ideal gas equation of state  $P_g = k_B n_g T_g$ , where  $T_g$  is the gas temperature. By assuming again that the hot gas is in hydrostatic equilibrium in the cluster, similarly to Eq. (33), a relation for the pressure of the hot gas as a function of the total mass of the cluster inside radius  $r$  is obtained as

$$\frac{1}{m_g n_g} \frac{d(n_g k_B T_g)}{dr} = \frac{k_B T_g}{\mu m_p} \left( \frac{1}{n_g} \frac{dn_g}{dr} + \frac{1}{T_g} \frac{dT_g}{dr} \right) = -\frac{GM(r)}{r^2}, \quad (36)$$

where  $m_g$  is the mass of the hot gas particle. For the mass of gas particle we take  $m_g = \mu m_p$  [21], where  $\mu = 0.61$ , and  $m_p$  is the proton mass.

When the hot interstellar gas density  $\rho_g$  and its temperature profile  $T_g$  are known from observations, the total mass within a radius  $r$  can be estimated by solving the equation of hydrostatic equilibrium Eq. (36). In spherical symmetry we obtain [38]

$$M(< r) = -\frac{k_B T_g r^2}{G \mu m_p} \left( \frac{1}{\rho_g} \frac{d\rho_g}{dr} + \frac{1}{T_g} \frac{dT_g}{dr} \right) = -\frac{k_B T_g r^2}{G \mu m_p} \frac{d}{dr} \ln [\rho_g(r) T_g(r)]. \quad (37)$$

## B. The isothermal gas case

If we adopt the isothermal condition for the hot gas  $T_g = \text{constant}$  from Eq. (36) we obtain

$$\frac{k_B T_g}{m_g n_g} \frac{dn_g}{dr} = -\frac{GM(r)}{r^2}. \quad (38)$$

Combining Eqs. (33), (35) and (38), we obtain the following relation between the condensed dark matter density  $\rho_{DM}$  and the hot gas parameters,

$$\frac{4\pi\hbar^2 a}{m^3} \frac{d\rho_{DM}}{dr} = \frac{k_B T_g}{m_g} \frac{d}{dr} (\ln n_g). \quad (39)$$

By integrating Eq. (39), it follows that the condensate dark matter density profile in galactic clusters is obtained as

$$\rho_{DM}(r) = \rho_{DM}(0) - \frac{3\beta m^3 k_B T_g}{8\pi m_g \hbar^2 a} \ln \left( 1 + \frac{r^2}{r_c^2} \right), \quad (40)$$

where  $\rho_{DM}(0)$  is the central dark matter density.

By introducing the cluster radius via the boundary condition requiring that  $\rho_{DM}(R) = 0$ , we obtain the radius of the cluster as a function of the central dark matter density  $\rho_{DM}(0)$  and the gas parameters as

$$R = r_c \sqrt{\exp \left[ \frac{8\pi m_g \hbar^2 a}{3\beta m^3 k_B T_g} \rho_{DM}(0) \right] - 1}, \quad (41)$$

or

$$R = r_c \sqrt{\exp \left[ 10^{-94} \times \frac{1 (a/\text{cm})}{\beta (m/g)^3} \frac{1}{(T/\text{keV})} \frac{\rho_{DM}(0)}{10^{-24} \text{g/cm}^3} \right] - 1}. \quad (42)$$

As a function of the cluster radius given by Eq. (41), the condensed dark matter density distribution in the cluster, Eq. (40), can be rewritten as

$$\rho_{DM}(r) = \frac{3\beta m^3 k_B T_g}{8\pi m_g \hbar^2 a} \ln \left( \frac{R^2 + r_c^2}{r^2 + r_c^2} \right), r \leq R. \quad (43)$$

Therefore, the total mass profile of the dark matter is

$$M_{DM}(r) = \int_0^r 4\pi (r')^2 \rho_{DM}(r') dr' = \bar{\rho} r_c^3 I \left( \frac{r}{r_c} \right), \quad (44)$$

where

$$I \left( \frac{r}{r_c} \right) = \int_0^{r/r_c} \xi^2 \ln \frac{1 + \xi_0^2}{1 + \xi^2} d\xi, \quad (45)$$

and

$$\xi_0 = \frac{R}{r_c}, \xi = \frac{r}{r_c}, \bar{\rho} = \frac{3\beta m^3 k_B T_g}{2 m_g \hbar^2 a} \quad (46)$$

The function  $I(r/r_c)$  can be obtained in an explicit form as

$$I \left( \frac{r}{r_c} \right) = \frac{2}{9} \left( \frac{r}{r_c} \right)^3 + \frac{1}{3} \left( \frac{r}{r_c} \right)^3 \ln \left( \frac{1 + \xi_0^2}{1 + r^2/r_c^2} \right) + \frac{2}{3} \tan^{-1} \left( \frac{r}{r_c} \right) - \frac{2}{3} \frac{r}{r_c}. \quad (47)$$



In both Eqs. (41) and (44), the unknown mass and scattering length of dark matter particle,  $m$  and  $a$  appear in the form of the combination  $m^3/a$ . In the following we consider a parameter  $\lambda$  that is defined as

$$\lambda = \left(\frac{m}{\text{g}}\right)^3 \left(\frac{a}{\text{cm}}\right)^{-1}, \quad (48)$$

and which fully describes the properties of the BEC condensed dark matter.

Remembering Eq. (27), the observed mass of a cluster is derived as [21]

$$M_{obs}(< r) = \frac{3k_B T_g r^3 \beta}{\mu m_p G} \frac{1}{r^2 + r_c^2}, \quad (49)$$

or

$$\frac{M_{obs}(r)}{10^{14} M_\odot} = 1.086 \times 10^{-3} \beta \left(\frac{T_g}{\text{keV}}\right) \frac{(r/\text{kpc})^3}{(r/\text{kpc})^2 + (r_c/\text{kpc})^2}. \quad (50)$$

By assuming that the total mass of the cluster is related to the dark matter by a relation of the form

$$M_{DM} = k_{DM}(M, n_g, T_g, \dots) M_{obs}, \quad (51)$$

where generally  $k_{DM}$  is a function of the total mass of the cluster, of the gas density, gas temperature etc., we obtain the parameter  $\lambda$  of the condensed dark matter as a function of the global parameters of the cluster ( $R, r_c$ ) as

$$\lambda = 2k_{DM}(M, n_g, T_g, \dots) \frac{\hbar^2}{G} \frac{1}{r_c^2} \left(\frac{R}{r_c}\right)^3 \frac{I^{-1}(R/r_c)}{1 + (R/r_c)^2}. \quad (52)$$

or

$$\lambda = 3.511 \times 10^{-90} \times k_{DM}(M, n_g, T_g, \dots) \times \left(\frac{r_c}{\text{kpc}}\right)^{-2} \times \left(\frac{R}{r_c}\right)^3 \frac{I^{-1}(R/r_c)}{1 + (R/r_c)^2} \text{g}^3/\text{cm}. \quad (53)$$

### 1. Numerical Analysis

The first step in the observational study of the galactic clusters is the determination of the integrated mass as a function of the radius  $r$  [21]. Once the integrated mass is known, one must define a physically meaningful fiducial radius for the mass measurement. There are two such radii used by astronomers to interpret observations, denoted as  $r_{200}$  and  $r_{500}$ , respectively. These radii are defined as the radii where the mean gravitational mass density of the matter  $\langle \rho_{tot} \rangle$  has the values  $\langle \rho_{tot} \rangle = 200\rho_{cr}$  and  $\langle \rho_{tot} \rangle = 500\rho_{cr}$ , respectively, with  $\rho_{cr}$ , representing the critical cosmological density given by  $\rho_{cr}(z) = 3H_0^2 h^2(z)/8\pi G$ , where  $h(z)$

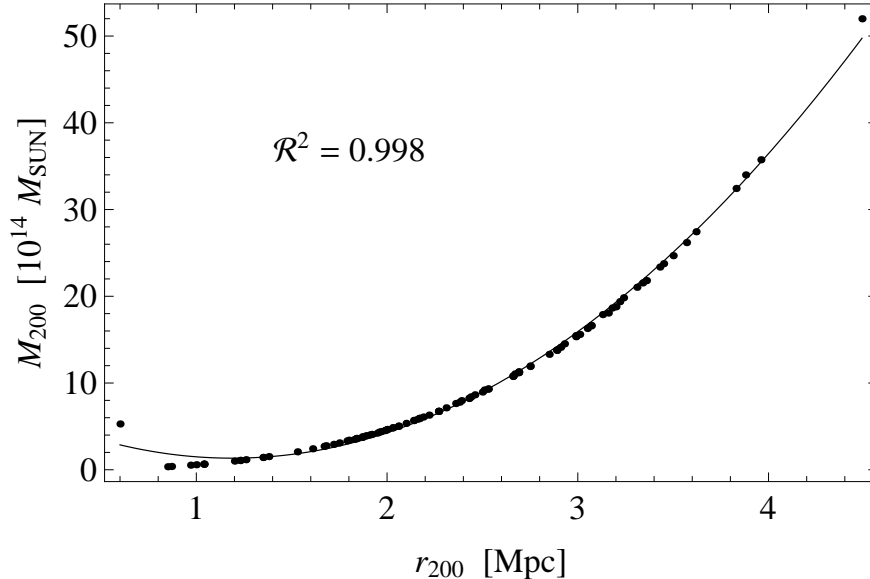


FIG. 1: Mass-radius relation for 106 clusters [21].

is the Hubble parameter normalized to its local value, i.e.,  $h^2(z) = \Omega_m(1+z)^3 + \Omega_\Lambda$ , where  $\Omega_m$  is the mass density parameter, and  $\Omega_\Lambda$  is the dark energy density parameter, respectively [32].  $H_0$  is the present day value of the Hubble function, and  $z$  denotes the cosmological redshift.

*a. The astrophysical data set* A generally used pragmatic approach for determining the virial mass  $M_{vir}$  of a galactic cluster is to use  $r_{200}$  as the outer boundary of the mass distribution in the cluster [21]. The numerical values of the cluster radius  $r_{200}$  are in the range  $r_{200} = 0.85$  Mpc (for the cluster NGC 4636) and  $r_{200} = 4.49$  Mpc (for the cluster A2163). Observations show that a typical value for  $r_{200}$  is approximately 2 Mpc [21]. The masses corresponding to  $r_{200}$  and  $r_{500}$  are denoted by  $M_{200}$  and  $M_{500}$ , respectively [21]. In the study of the gravitational dynamics of galaxy clusters it is usually assumed that  $M_{vir} \approx M_{200}$  and  $R_{vir} \approx r_{200}$ , where  $R_{vir}$  denotes the virial radius of the cluster [21].

In the following we will use the observational data presented in [21]. The mass-radius and mass-temperature dependencies of the considered clusters are presented in Figs. 1 and 2, respectively, where  $M_{200}$ ,  $R_{200}$  and  $T_X$  are data corresponding to each of the 106 clusters analyzed in [21].

The observational data can be fitted with some simple functions, which allows to obtain

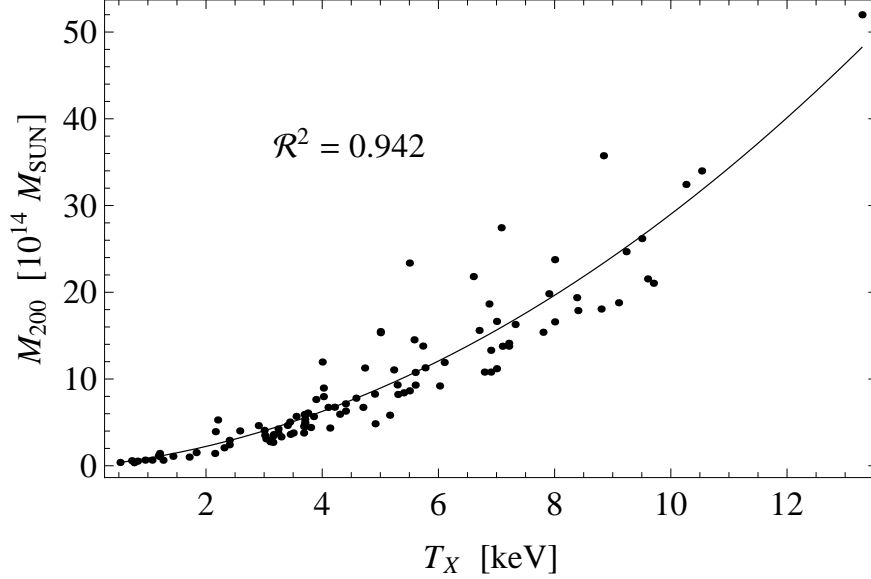


FIG. 2: Cluster mass-gas temperature relation for 106 clusters [21].

the cluster mass-cluster radius relation in the form

$$\frac{M_{200}}{10^{14}M_{\odot}} = 4.439 \left( \frac{r_{200}}{\text{Mpc}} \right)^2 - 10.545 \left( \frac{r_{200}}{\text{Mpc}} \right) + 7.599, \quad (54)$$

with a correlation coefficient  $\mathcal{R}^2 = 0.998$ . The cluster mass - hot intracluster gas temperature relation can be obtained analytically as

$$\frac{M_{200}}{10^{14}M_{\odot}} = 0.221 \left( \frac{T_X}{\text{keV}} \right)^2 + 0.690 \left( \frac{T_X}{\text{keV}} \right) - 0.038, \quad (55)$$

with a correlation coefficient  $\mathcal{R}^2 = 0.942$ .

In the following we neglect the mass of the cluster bulge and the cluster disc as their masses ( $M_b, M_d \sim 10^{10}M_{\odot}$ ) are much smaller than the dark matter mass [43]. With this in mind, we shall assume that the dark matter accounts for most of the mass (around 90%) of the cluster.

*b. The physical parameter  $\lambda$  of the dark matter particle* Consider the definition of  $\lambda$ , given by Eq. (53), in the context of the observational data provided by analysis of the 106 clusters. For each of these clusters  $\lambda$  takes a different value,  $\lambda_i$ . Following a simple averaging, with the use of the observational data of [21] we obtain

$$\langle \lambda \rangle = \sum_{i=1}^n \frac{\lambda_i}{n} = 4.27969 \times 10^{-96} \text{ g}^3/\text{cm}, \quad (56)$$

for  $k_{DM} = 0.9$ , while

$$\frac{\langle \lambda \rangle}{k_{DM}} = 4.75522 \times 10^{-96} \text{ g}^3/\text{cm}. \quad (57)$$

In a different approach, one can fit the results of Eq. (44), representing the theoretical prediction for the dark matter mass, for each of the clusters with the observed cluster mass data in [21]. This is a straightforward problem once one notices that, with the help of Eq. (53) and the definition of  $\bar{\rho}$  from Eq. (46), the theoretical expression for the dark matter mass may be written as

$$M_{DM} = \lambda x, \quad x = \frac{3\beta}{2m_g} \frac{k_B T_g}{\hbar^2} r_c^3 I \left( \frac{r}{r_c} \right).$$

By considering that the observational mass  $M_{200}$  is a vector  $y$ , the problem becomes to find the parameter  $\lambda$  which produces the best fit of the equation  $\lambda x$  to  $y$ . The standard approach to solving such a problem is the least squares method [22], i.e. find  $\lambda$  which minimises  $\sum_i^n (y_i - \lambda x_i)^2$ . To this end, we define a function

$$Z_M^2 = \sum_{i=1}^n [M_{200}^i - M_{DM}^i(r_{200})]^2 \quad (58)$$

where  $M_{DM}^i(R)$  is obtained from Eq. (44). Please be aware that the standard notation for this function is  $R^2$ . We chose to denote it  $Z^2$  so as to avoid confusion with the different radii used in the paper. The value of  $\lambda$  which minimises the function  $Z_M^2$  is found to be

$$\lambda_0 = 1.76624 \times 10^{-96} \text{ g}^3/\text{cm}. \quad (59)$$

Similarly, two different approaches may be used to find the central density of the dark matter. First, by using Eq. (41) with  $R \equiv r_{200}$ , we can find, for each cluster (with fixed  $\lambda_0$ ), a value  $\rho_{DM}^i(0)$ , and thus a mean value

$$\langle \rho_{DM}(0) \rangle = \sum_{i=1}^n \frac{\rho_{DM}^i(0)}{n} = 4.86714 \times 10^{-13} \text{ g}/\text{cm}^3. \quad (60)$$

In order to find the value of  $\rho_{DM}(0)$  that best fits the entire data set, we use Eq. (41), and define the functions

$$F_i = \log \left\{ \left( \frac{r_{200}^i}{r_c^i} \right)^2 + 1 \right\}, \quad G_i = \frac{8\pi}{3\beta_i} \frac{m_g}{m^3} \frac{\hbar^2 a}{k_B T_g^i} \rho_{DM}(0), \quad (61)$$

and

$$Z_R^2 = \sum_{i=1}^n (F_i - G_i)^2, \quad (62)$$

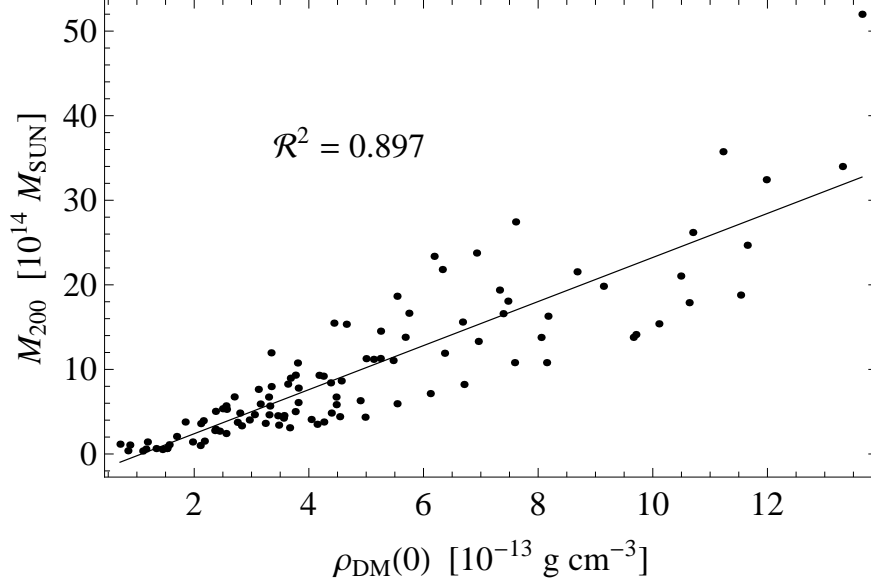


FIG. 3: Predicted mass-central density relation for 106 clusters, in the case of the isothermal intracluster gas model.

respectively. The value of  $\rho_{DM}(0)$  which extremises  $Z_R^2$  is

$$\rho_{DM}^{(0)}(0) = 1.90934 \times 10^{-13} \text{ g/cm}^3, \quad (63)$$

for fixed  $m^3/a = \lambda_0$ .

With these results, the plots of the cluster mass-cluster central density and hot gas temperature-cluster central density relations are shown in Figs. 3 and 4. Fitting an equation of the type  $ax + b$  gives the remarkably simple relations

$$\frac{M_{200}}{10^{14} M_{\odot}} = 2.604 \frac{\rho_{DM}(0)}{10^{-13} \text{ g/cm}^3} - 2.812, \quad (64)$$

with a correlation coefficient  $\mathcal{R}^2 = 0.897$  for the cluster mass-cluster central density relation, and

$$\frac{T_X}{\text{keV}} = 0.798 \frac{\rho_{DM}(0)}{10^{-13} \text{ g/cm}^3} + 0.930, \quad (65)$$

with  $\mathcal{R}^2 = 0.973$  for the intracluster gas temperature-cluster central density relation, respectively.

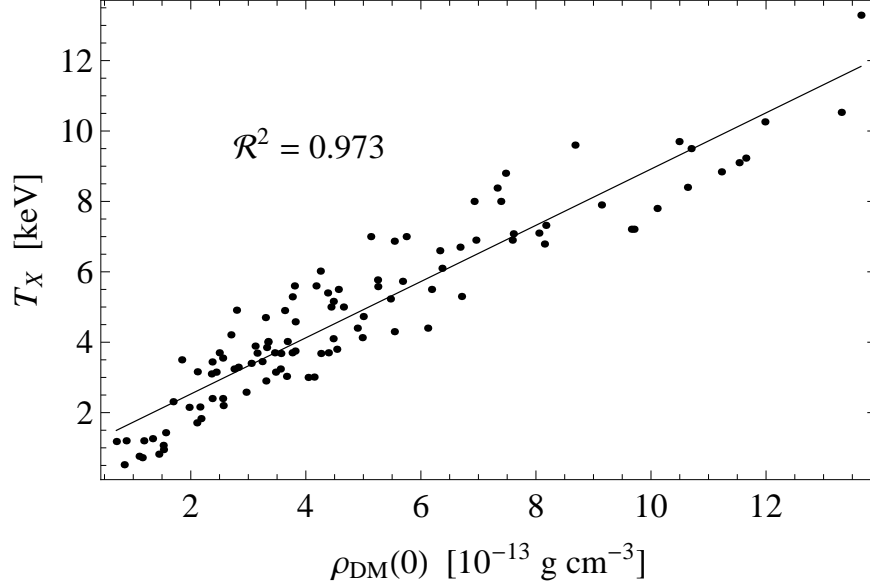


FIG. 4: Predicted gas temperature-central density relation for 106 clusters, in the case of the isothermal intracluster gas model.

2. *Astrophysical implications: limits on the mass and scattering length of the BEC dark matter particles*

An important characteristic of the dark matter particles is their self-interaction cross-section, defined as

$$\sigma_m = \frac{4\pi a^2}{m}. \quad (66)$$

Recent observations [6], as well as numerical simulations of the merging galaxy cluster 1E 0657-56 (the Bullet cluster) [30], have suggested an upper limit (68% confidence for simulations) for  $\sigma_m$  of the order of  $\sigma_m < 1.25 \text{ cm}^2/\text{g} = 2.23 \times 10^{-7} \text{ fm}^2/\text{eV}$ . By combining Eq. (53), giving the definition of the parameter  $\lambda$ , with Eq. (66), we can obtain the mass and scattering length of the BEC dark matter particles as

$$m = \sqrt[5]{\frac{\lambda_0^2 \sigma_m}{4\pi}} < 4.4583 \times 10^{-39} \text{ g} = 1.7638 \times 10^{-3} \text{ meV}, \quad (67)$$

$$a = \sqrt[5]{\frac{\lambda_0 \sigma_m^3}{(4\pi)^3}} < 1.7702 \times 10^{-20} \text{ cm} = 1.7702 \times 10^{-7} \text{ fm}, \quad (68)$$

where for the numerical estimations we have considered the upper limits of  $\sigma_m$  and  $\lambda$ . Thus, the presented numerical values give the upper limits for the mass and scattering length of the dark matter particles. The upper limit of BEC dark matter particle mass is a little bit

smaller than the region that QCD predicts for the mass of the axion,  $6.0 \mu\text{eV} < m < 2.0 \text{ meV}$  [34]. This upper limit is also smaller than the result in [35] that the axion mass is of the order of  $m = 0.11 \text{ meV}$ . The value of the scattering length obtained from the cross section of the self-interacting dark matter and zero-temperature approximation, is much smaller than the value of  $a = 10^4 - 10^6 \text{ fm}$  obtained in laboratory experiments on atomic BECs [12].

#### IV. THE EFFECT OF THE INTRACLUSTER HOT GAS TEMPERATURE VARIATION ON THE BEC DARK MATTER DENSITY PROFILE

In the previous Section we have considered that the intracluster gas is isothermal,  $T_g = \text{constant}$ , and there are no temperature variations in the gas temperature. However, a large number of astrophysical investigations have shown that the gas temperature structure on Mpc scales is highly complex and non-isothermal [36–43]. Through a detailed analysis of the observational data of a sample of hot nearby clusters it was found that the gravitating mass within 1 and 6 times core radius are approximately within 1.35 and 0.7 times that the isothermal  $\beta$ -model estimates [36]. From the analysis of the temperature of 13 galaxy clusters a scaled temperature profile of the form  $T/\langle T \rangle = 1.07, 0.035 < r/r_{180} < 0.125$ ,  $T/\langle T \rangle = 1.22 - 1.2r/r_{180}, 0.125 < r/r_{180} < 0.6$  was obtained in [39], where  $r_{180} = 2.74 \text{ Mpc} (\langle T \rangle / 10 \text{ keV})^{1/2}$  is the cluster’s virial radius [40]. As for the central region ( $r/r_{180} < 0.035$ ) of the cluster, the temperature profiles scatter since non-gravitational processes such as radiative cooling and energy output are important. Hence, in order to obtain a realistic description of the galaxy cluster properties one should take into account in the left hand side of Eq. (36) the presence of the temperature gradients in the hot intracluster gas.

On the other hand in [44] it was suggested that the temperature variations may only amount to 20-30% ( $T_g dn_g/dr \sim 4 - 5$  times greater than  $n_g dT_g/dr$ ), thus having little effect on the astrophysical parameters of the cluster.

In order to examine the effect of the intracluster gas temperature variations on the Bose-Einstein Condensate dark matter properties we adopt a very simple model for the temperature variations, described by the equation [36, 37],

$$T_g(r) = \frac{T_0}{[1 + (r/r_c)^2]^\delta}, \quad (69)$$

where  $T_0 = T(0)$  is the gas temperature at the cluster center, and  $\delta = 3\beta(\gamma - 1)/2$ , where

$\beta = 2/3$  and  $\gamma = 1.24_{-0.12}^{+0.20}$ . Therefore in the presence of gas temperature gradients the BEC dark matter profile is given by the equation

$$\frac{4\pi\hbar^2 a}{m^3} \frac{d\rho_{DM}(r)}{dr} = \frac{k_B T_g(r)}{\mu m_p} \frac{d}{dr} [\ln n_g(r) T_g(r)]. \quad (70)$$

By taking into account the explicit expressions of the gas particle density and of the temperature, given by Eqs. (35) and (69), respectively, we obtain first

$$\frac{4\pi\hbar^2 a}{m^3} \frac{d\rho_{DM}(r)}{dr} = -\frac{3\beta\gamma k_B T_0}{\mu m_p r_c^2} r \left(1 + \frac{r^2}{r_c^2}\right)^{-3\beta(\gamma-1)/2-1}, \quad (71)$$

giving the BEC dark matter density profile as

$$\rho_{DM}(r) = C + \frac{\gamma}{4\pi(\gamma-1)\mu} \frac{m^3 k_B T_0}{m_p \hbar^2 a} \left(1 + \frac{r^2}{r_c^2}\right)^{-3\beta(\gamma-1)/2}, \quad (72)$$

where  $C$  is an arbitrary integration constant. Since

$$\rho_{DM}(0) = C + \frac{\gamma m^3 k_B T_0}{4\pi(\gamma-1)\mu m_p \hbar^2 a}, \quad (73)$$

it follows that finally the dark matter density profile is obtained as

$$\rho_{DM}(r) = \rho_{DM}(0) - \frac{\gamma}{4\pi(\gamma-1)\mu} \frac{m^3 k_B T_0}{m_p \hbar^2 a} \left[1 - \left(1 + \frac{r^2}{r_c^2}\right)^{-3\beta(\gamma-1)/2}\right]. \quad (74)$$

The radius of the cluster is obtained from the condition  $\rho_{DM}(r) = 0$ , giving

$$R = r_c \sqrt{\left[1 - \frac{4\pi(\gamma-1)\mu}{\gamma} \frac{m_p \hbar^2 a}{m^3 k_B T_0} \rho_{DM}(0)\right]^{-2/[3\beta(\gamma-1)]} - 1}, \quad (75)$$

and

$$\rho_{DM}(r) = \frac{\gamma}{4\pi(\gamma-1)\mu} \frac{m^3 k_B T_0}{m_p \hbar^2 a} \left[ \left(1 + \frac{r^2}{r_c^2}\right)^{-3\beta(\gamma-1)/2} - \left(1 + \frac{R^2}{r_c^2}\right)^{-3\beta(\gamma-1)/2} \right], \quad (76)$$

respectively.

The total dark matter mass of the cluster is obtained from  $M_{DM}(r) = 4\pi \int_0^r \rho_{DM}(r') r'^2 dr'$ , and is represented by the relation

$$M_{DM}(r) = \frac{\gamma}{3(\gamma-1)\mu} \frac{m^3 k_B T_0}{m_p \hbar^2 a} r^3 \left[ {}_2F_1 \left( \frac{3}{2}, \frac{3}{2}\beta(\gamma-1); \frac{5}{2}; -\frac{r^2}{r_c^2} \right) - \left(1 + \frac{R^2}{r_c^2}\right)^{-\frac{3}{2}\beta(\gamma-1)} \right], \quad (77)$$

where the hypergeometric function  ${}_2F_1(a, b; c; z)$  is defined as  ${}_2F_1(a, b; c; z) = \sum_{k=0}^{\infty} (a)_k (b)_k (c)_k z^k / k!$ .



With the use of Eq. (27) we obtain the total mass of the cluster in the present varying gas temperature model as

$$M(r) = \frac{3\beta\gamma}{\mu m_p} \frac{k_B T_0}{G} \frac{1}{r_c^2} r^3 \left(1 + \frac{r^2}{r_c^2}\right)^{-3\beta(\gamma-1)/2-1}. \quad (78)$$

By assuming that the BEC dark matter mass is proportional to the total mass, with the proportionality coefficient denoted again by  $k_{DM} = k_{DM}(M, T_0, \dots)$ , we obtain for the parameter  $\lambda$  describing the condensate physical properties the expression

$$\lambda = 4.5 k_{DM} \beta (\gamma - 1) \frac{\hbar^2}{G} \frac{1}{r_c^2} \frac{(1 + R^2/r_c^2)^{-3\beta(\gamma-1)/2-1}}{{}_2F_1(3/2, 3\beta(\gamma-1)/2; 5/2; -R^2/r_c^2) - \left(1 + \frac{R^2}{r_c^2}\right)^{-3\beta(\gamma-1)/2}}. \quad (79)$$

Applying the same type of numerical procedure as presented for the isothermal case, with  $\gamma = 1.24$ , Eq. (79) provides

$$\langle \lambda \rangle = 3.65389 \times 10^{-96} \text{ g}^3/\text{cm}, \quad (80)$$

for  $k_{DM} = 0.9$  and

$$\frac{\langle \lambda \rangle}{k_{DM}} = 4.05987 \times 10^{-96} \text{ g}^3/\text{cm}, \quad (81)$$

respectively. A fit of the observational data with respect to Eq. (77) leads to a value of

$$\lambda_1 = 4.20896 \times 10^{-96} \text{ g}^3/\text{cm}, \quad (82)$$

which extremises the  $Z_M^2$  function.

By replacing  $R$  with  $r_{200}$  from Eq. (75) one can extract the value of  $\rho_{DM}(0)$  for each cluster. Thus we obtain  $\langle \rho_{DM}(0) \rangle = 8.19759 \times 10^{-13} \text{ g}/\text{cm}^3$ . To obtain a value of the central density that is a best fit for the entire set of data, we use Eq. (75), and define the functions

$$F_i = \left[ \left( \frac{R_{200}^i}{r_c^i} \right)^2 + 1 \right]^{-3\beta_i(\gamma-1)/2}, \quad G_i = 1 - \frac{4\pi(\gamma-1)\mu m_p}{\gamma} \frac{\hbar^2 a}{m^3 k_B T_i} \rho_{DM}(0), \quad (83)$$

and

$$Z_R^2 = \sum_{i=1}^n (F_i - G_i)^2, \quad (84)$$

respectively. The value of  $\rho_{DM}(0)$  which extremises  $Z_R^2$  is  $\rho_{DM}^{(1)}(0) = 4.10184 \times 10^{-13} \text{ g}/\text{cm}^3$  for fixed  $m^3/a = \lambda_1$ .

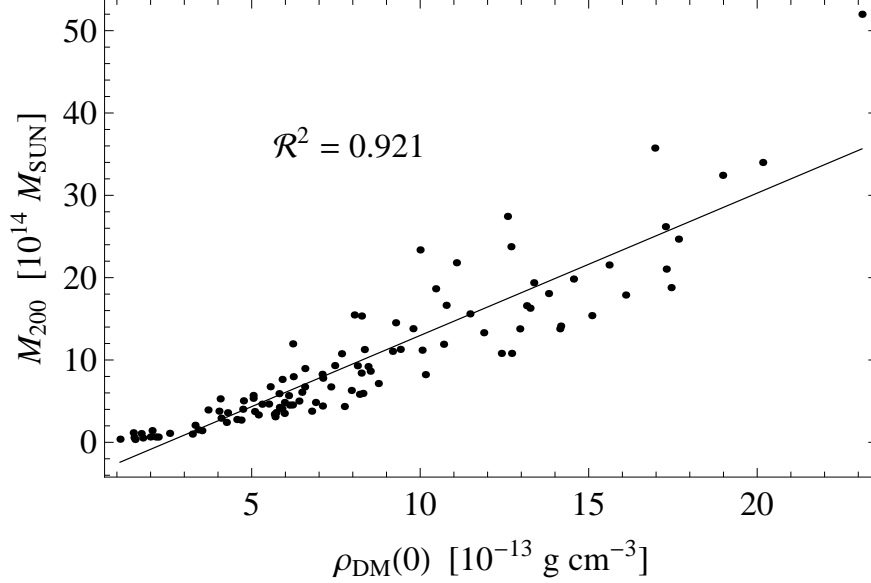


FIG. 5: Cluster mass-central density relation for 106 clusters, for the non-isothermal intracluster gas model.

With these results, the plots of the cluster mass-central density and hot gas temperature-central density relations are shown in Figs. 5 and 6. Fitting an equation of the type  $ax + b$ , produces

$$\frac{M}{10^{14} M_{\odot}} = 1.728 \frac{\rho_{DM}(0)}{10^{-13} \text{ g/cm}^3} - 4.306, \quad (85)$$

with  $\mathcal{R}^2 = 0.921$  for the cluster mass-cluster central density relation, and

$$\frac{T_X}{\text{keV}} = 5.358 \frac{\rho_{DM}(0)}{10^{-13} \text{ g/cm}^3} + 0.425, \quad (86)$$

with  $\mathcal{R}^2 = 0.991$  for the hot gas temperature-cluster central density relation.

A simple qualitative estimate of the effect of the gas temperature on the dark matter profile can be obtained by considering an upper limit in the relation between the temperature gradient and the density gradient in the gas. By assuming that the contribution of the temperature gradient is approximately as much as half of the one of the number density gradient, we obtain

$$n_g \frac{dT_g}{dr} \sim 50\% T_g \frac{dn_g}{dr}, \quad (87)$$

and the dark matter density becomes

$$\rho_{DM}(r) = 1.5 \times \frac{3k_B T_g \beta m^3}{8\pi \hbar^2 m_g a} \ln \left( \frac{R^2 + r_c^2}{r^2 + r_c^2} \right) \quad (88)$$

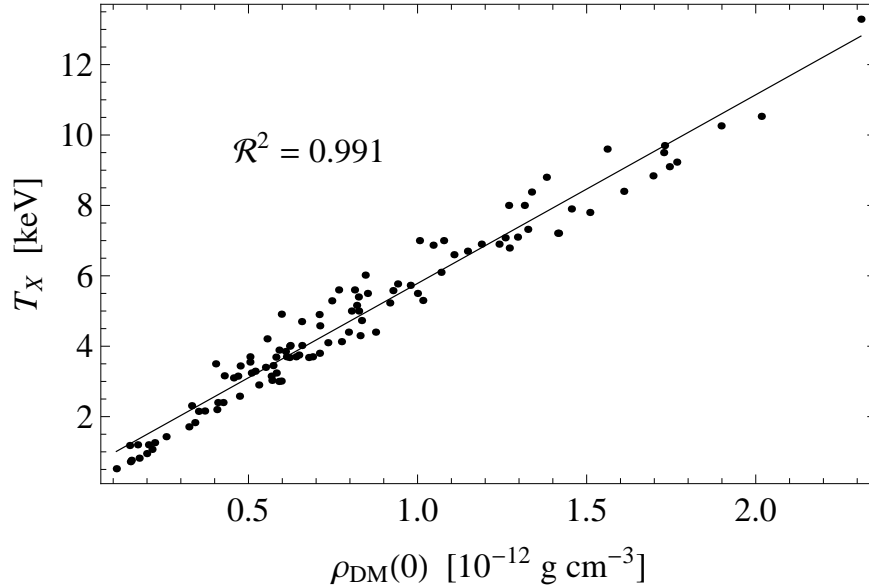


FIG. 6: Gas temperature-central density relation for 106 clusters, for the non-isothermal intracluster gas model.

Still, detailed temperature profiles and other non-gravitational factors in the core regions are needed to derive a more accurate density profile of dark matter.

To sum up, due to a lack of knowledge about the temperature profiles in most clusters and on the role of the important effects of non-gravitational factors on the cluster hot gas, there are still many uncertainties in the derivation of the dark matter density profile by using gravitational methods.

## V. THE FINITE TEMPERATURE BOSE-EINSTEIN CONDENSATE DARK MATTER MODEL

Unlike the zero temperature BEC dark matter model, in which all bosons stay in the condensed phase, in the finite temperature BEC model, at least, a fraction of the particles can be found in the thermal cloud (non-condensed) phase). According to a fundamental relation of statistical physics, the ratio of the number of the condensed particles  $N_0$  and the total particle number  $N$  is given by the relation [23, 25]

$$\frac{\langle N_0 \rangle}{N} = 1 - \left( \frac{T}{T_{tr}} \right)^\gamma \quad (89)$$

where  $\gamma = 3/2$  in ideal gas BEC and  $\gamma = 3$  in gas BEC trapped by harmonic potential. When  $T = 0$  all the particles are in the condensed phase. In the following we will consider the effects of the finite temperature of the BEC dark matter on the astrophysical properties of the galactic clusters.

### A. Astrophysical parameters of the finite temperature BEC dark matter in the presence of a thermal cloud

In the following we denote by  $(\rho_c, p_c)$  and  $(\tilde{\rho}, \tilde{p})$  the energy densities and pressures of the dark matter in the condensed and non-condensed (thermal cloud) phases. Moreover, we introduce the dimensionless condensate density  $\theta(r)$ , related to the condensate density by the relation

$$\rho_c(r) = \rho_{tr} \frac{2^{2/3} m^{1/3}}{a} \theta(r) = \rho_{tr} \kappa \theta(r), \quad (90)$$

where we have denoted  $\kappa = m^{1/3}/\rho_{tr}^{1/3} a$ . In the following we also denote  $t = T/T_{tr}$ .

By considering that both the condensed and the non-condensed bosonic phases are in chemical potential equilibrium, the total energy density  $\rho_{DM} = \rho_c + \tilde{\rho}$  and the total pressure  $p_{DM} = p_c + \tilde{p}$  can be expressed in the form of power expansions in the dimensionless condensate density as [18]

$$\begin{aligned} \rho_{DM}(t, \theta) &= \rho_{tr} \left[ \kappa \theta + t^{3/2} - 2.642t\sqrt{\theta} + 2.120t^{1/2}\theta - 0.572t^{-1/2}\theta^2 + 0.088t^{-3/2}\theta^3 \right], \\ p_{DM}(t, \theta) &= p_{tr} \left[ 0.513t^{5/2} - 3.793t^{3/2}\theta + 0.004t\theta^{3/2} + \left( 1.896\kappa + 4.021\sqrt{t} \right) \theta^2 - \right. \\ &\quad \left. \frac{2.139\theta^3}{\sqrt{t}} + \frac{0.504\theta^4}{t^{3/2}} \right], \end{aligned} \quad (91)$$

where we have denoted

$$p_{tr} = \rho_{tr} \frac{k_B T_{tr}}{m}. \quad (92)$$

Then, by assuming that both non-condensate and condensate dark matter are bound in hydrostatic equilibrium by the total mass profile, we obtain

$$\frac{1}{\rho_{DM}} \frac{d\rho_{DM}}{dr} = \frac{k_B T_g}{m_g} \frac{d(\ln n_g)}{dr} = -\frac{3\beta k_B T_g}{m_g r_c^2} \frac{r}{(1 + r^2/r_c^2)}, \quad (93)$$

where we have assumed that the intracluster gas is isothermal,  $T_g = \text{constant}$ . In the following we introduce the dimensionless variable  $\xi = r/r_c$ , and we denote

$$\alpha = \frac{3\beta}{\mu} \frac{m}{m_p} \frac{T_g}{T_{tr}}. \quad (94)$$

Therefore the equation describing the finite temperature bosonic dark matter profile in a galactic cluster is given by

$$\frac{2.016\theta^3 + (3.792\kappa t^{3/2} + 8.04t^2)\theta + 0.006t^{5/2}\sqrt{\theta} - 3.793t^3 - 6.417t\theta^2}{0.088\theta^3 + kt^{3/2}\theta - 2.642t^{5/2}\sqrt{\theta} + t^3 + 2.12t^2\theta - 0.572\sqrt{t}\theta^2} \frac{d\theta}{d\xi} = -\frac{\alpha\xi}{1 + \xi^2}. \quad (95)$$

Eq. (95) must be integrated with the initial condition  $\theta(0) = \theta_0$ , a condition which gives the value of the Bose-Einstein condensed dark matter at the galactic cluster's center. The mass distribution of the dark matter can be obtained from the equation

$$\frac{dm}{d\xi} = \xi^2 \left[ \kappa\theta + t^{3/2} - 2.642t\sqrt{\theta} + 2.120t^{1/2}\theta - 0.572t^{-1/2}\theta^2 + 0.088t^{-3/2}\theta^3 \right], \quad (96)$$

where

$$m(\xi) = \frac{M(\xi)}{4\pi r_c^3 \rho_{tr}}. \quad (97)$$

The initial condition for Eq. 96) is  $m(0) = 0$ . The variations of the total density of the finite temperature dark matter, of its pressure, and of the dark matter mass distribution in the cluster are presented, for fixed  $\kappa$ ,  $\alpha$ , and  $\theta_0$ , and for different values of  $t$ , in Figs. 7-9.

## B. Finite temperature BEC dark matter: neglecting the effect of the thermal excitations

In the following we consider a simplified finite temperature dark matter BEC model, in which we assume that the effects of the thermal excitations can be neglected. Thus, we assume that  $\rho_c \gg \tilde{\rho}$ , and  $p_c \gg \tilde{p}$ . These conditions imply that the dark matter temperature is close to the absolute zero temperature. Moreover, we assume that the BEC dark matter is isothermal, that is, its temperature  $T$  is a constant inside the cluster. In terms of the dimensionless density  $\theta$ , defined by Eq. (90), from Eq. (25) we obtain for the thermodynamic pressure of the finite temperature BEC dark matter the expression

$$p_c(T, \theta) = \rho_{tr} \frac{k_B T_{tr}}{m} \left[ 1.896\kappa\theta^2 - 6.680 \left( \frac{T}{T_{tr}} \right) \theta^{3/2} + 8.043 \left( \frac{T}{T_{tr}} \right)^{1/2} \theta^2 - 2.863 \left( \frac{T}{T_{tr}} \right)^{-1/2} \theta^3 + 0.504 \left( \frac{T}{T_{tr}} \right)^{-3/2} \theta^4 \right]. \quad (98)$$

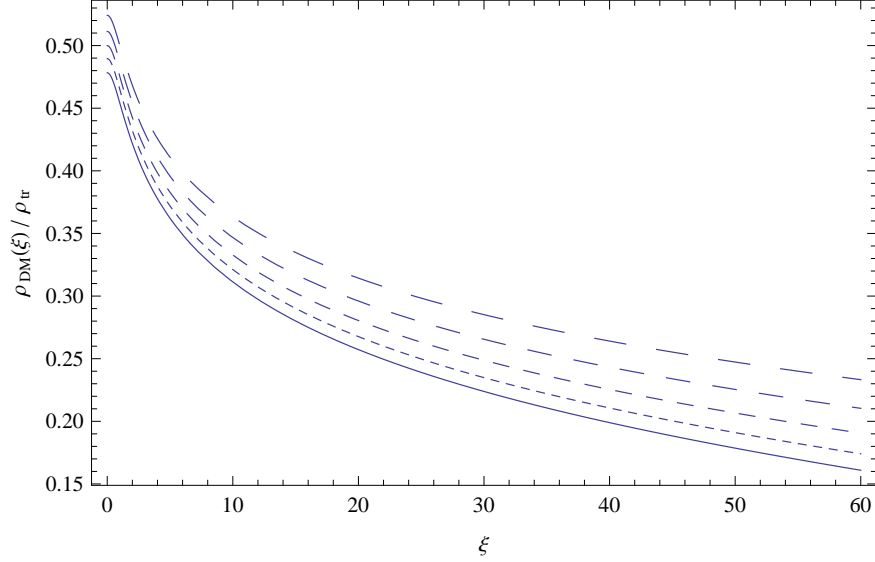


FIG. 7: Variation of the finite temperature bosonic dark matter dimensionless density profile  $\rho_{DM}/\rho_{tr}$  for  $\kappa = 5$ ,  $\alpha = 0.06$ , and for different values of  $t = T/T_{tr}$ :  $t = 0.15$  (solid curve),  $t = 0.20$  (dotted curve),  $t = 0.25$  (short dashed curve),  $t = 0.30$  (dashed curve), and  $t = 0.35$  (long dashed curve), respectively. The central value of the Bose-Einstein Condensed dark matter is  $\theta(0) = 0.10$ .

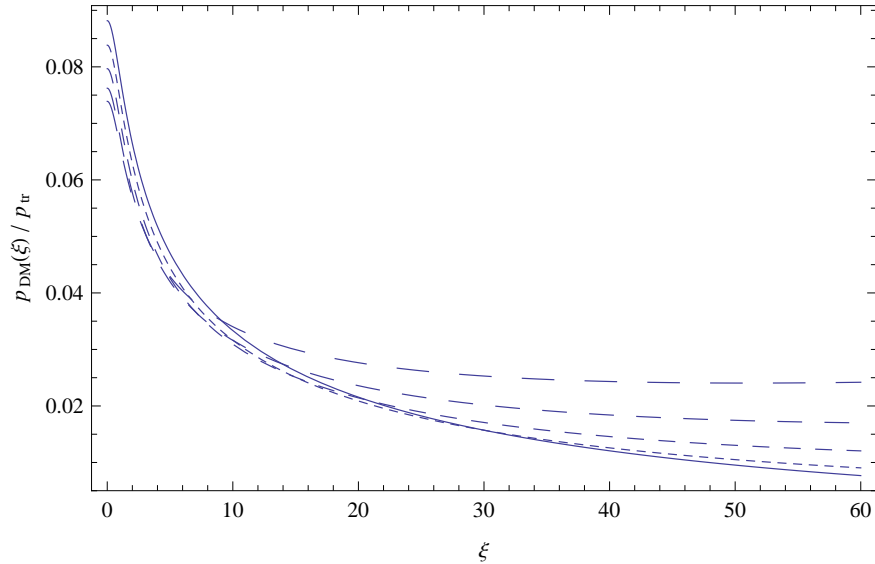


FIG. 8: Dimensionless pressure profile  $p_{DM}/p_{tr}$  of the finite temperature bosonic dark matter for  $\kappa = 5$ ,  $\alpha = 0.06$ , and for different values of  $t = T/T_{tr}$ :  $t = 0.15$  (solid curve),  $t = 0.20$  (dotted curve),  $t = 0.25$  (short dashed curve),  $t = 0.30$  (dashed curve), and  $t = 0.35$  (long dashed curve), respectively. The central value of the Bose-Einstein Condensed dark matter is  $\theta(0) = 0.10$ .

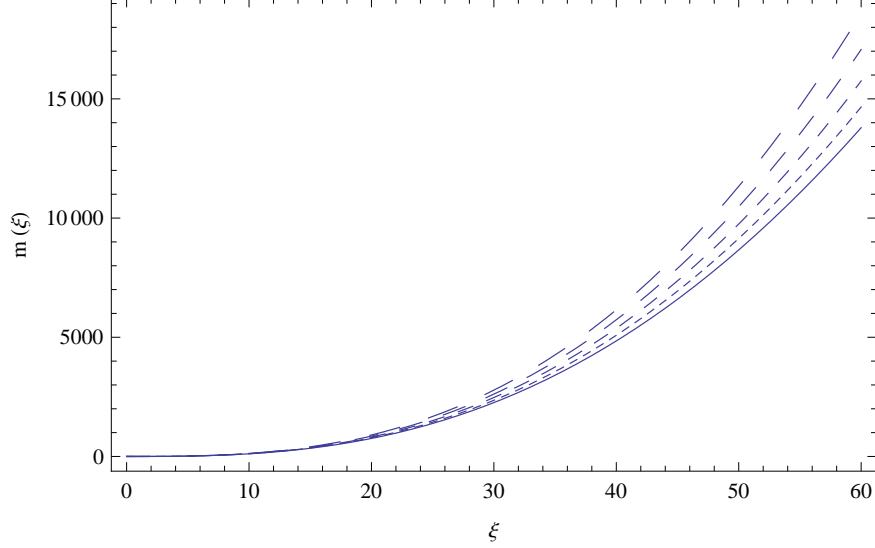


FIG. 9: Dimensionless mass profile  $m(\xi)$  of the finite temperature bosonic dark matter for  $\kappa = 5$ ,  $\alpha = 0.06$ , and for different values of  $t = T/T_{tr}$ :  $t = 0.15$  (solid curve),  $t = 0.20$  (dotted curve),  $t = 0.25$  (short dashed curve),  $t = 0.30$  (dashed curve), and  $t = 0.35$  (long dashed curve), respectively. The central value of the Bose-Einstein Condensed dark matter is  $\theta(0) = 0.10$ .

The ratio  $p_c/p_0$  for the condensate, where  $p_0$  is the central pressure, is determined by the numerical value of the dimensionless parameter  $\kappa = m^{1/3}/\rho_{tr}^{1/3}a$ . By assuming that the intracluster gas is isothermal with  $T_g = \text{constant}$ , and in gravitational equilibrium inside the cluster, we obtain the basic equation describing the density distribution of the finite temperature BEC dark matter as

$$\frac{k_B T_g}{\mu m_p} \frac{d}{dr} \ln n_g = \frac{1}{\rho_c} \frac{dp_c}{dr}, \quad (99)$$

giving immediately after integration

$$C - \frac{3\beta k_B T_g}{2\mu m_p} \ln \left( 1 + \frac{r^2}{r_c^2} \right) = \frac{k_B T_{tr}}{\kappa m} \left[ -20.04t\theta^{1/2} + \left( 3.792\kappa + 16.08\sqrt{t} \right) \theta - 4.294t^{-1/2}\theta^2 + 0.672t^{-3/2}\theta^3 \right], \quad (100)$$

respectively, where  $C$  is an arbitrary constant of integration, which is determined by the central density of the cluster. Since  $\theta \ll 1$ , in the limit of finite  $t$  the last two terms in Eq. (100) can be neglected as being negligibly small. In the zeroth order approximation of

the zero temperature limit of the BEC dark matter we obtain first

$$\theta^{(0)}(r) = \theta^{(0)}(0) - \frac{3\beta}{7.584\mu} \frac{m}{m_p} \frac{T_g}{T_{tr}} \ln \left( 1 + \frac{r^2}{r_c^2} \right), \quad (101)$$

where  $\theta^{(0)}(0) = mC/3.792k_B T_{tr}$  is the central value of the dimensionless density of the cluster. This relation also gives the value of the integration constant  $C$  in terms of the central value of the dimensionless density  $\theta$ . At this moment we can define the radius  $R$  of the cluster from the condition  $\theta^{(0)}(R) = 0$ , which gives for the central value of  $\theta$  the expression  $\theta^{(0)}(0) = (3\beta/7.584\mu) (m/m_p) (T_g/T_{tr}) \ln(1 + R^2/r_c^2)$ .

In the first order of approximation we have

$$\theta(r) = \theta^{(0)}(r) + \theta^{(1)}(r), \quad (102)$$

where  $\theta^{(1)}(r) \ll \theta^{(0)}(r)$ ,  $\forall r \in [0, R]$ . After substitution in Eq. (100) we obtain for  $\theta^{(1)}(r)$  the expression

$$\theta^{(1)}(r) = \frac{20.04t - 16.08\sqrt{t}}{3.792\kappa - 10.02t + 16.08\sqrt{t}} \theta_0 \approx \left[ -\frac{4.24051\sqrt{t}}{\kappa} + \frac{(5.28481\kappa + 17.9819)t}{\kappa^2} \right] \theta_0. \quad (103)$$

Therefore for the finite temperature Bose-Einstein Condensate dark matter density and mass distribution we obtain the expressions

$$\rho_{DM}^{(T)}(r, T) \approx \frac{3\beta}{8\pi} \frac{\lambda}{m_g} \frac{k_B T_g}{\hbar^2} \left[ 1 - \frac{4.24051\sqrt{t}}{\kappa} + \frac{(5.28481\kappa + 17.9819)t}{\kappa^2} \right] \ln \left( \frac{R^2 + r_c^2}{r^2 + r_c^2} \right), \quad r \leq R, \quad (104)$$

and

$$M_{DM}^{(T)}(r, T) \approx \bar{\rho}_T r_c^3 I \left( \frac{r}{r_c} \right), \quad (105)$$

respectively, where

$$\bar{\rho}_T = \frac{3\beta}{2} \frac{m^3}{m_g} \frac{k_B T_g}{\hbar^2 a} \left[ 1 - \frac{4.24051\sqrt{t}}{\kappa} + \frac{(5.28481\kappa + 17.9819)t}{\kappa^2} \right]. \quad (106)$$

In the present order of approximation the radius  $R$  of the cluster is not affected by the physical effects related to the finite temperature of the BEC dark matter.

By fixing the value of  $\lambda$  to the one obtained as a best fit for the case of zero temperature BEC in an isothermal gas,  $\lambda_0 = 1.76624 \times 10^{-96} \text{ g}^3/\text{cm}$  we explore the parameter space  $\{t, \kappa\}$  needed to extremise the values of the function  $Z_M^2$ , defined in this case for the dark matter mass as given by Eq. (105). A plot of the variation of these parameters for two values of  $\lambda$ ,



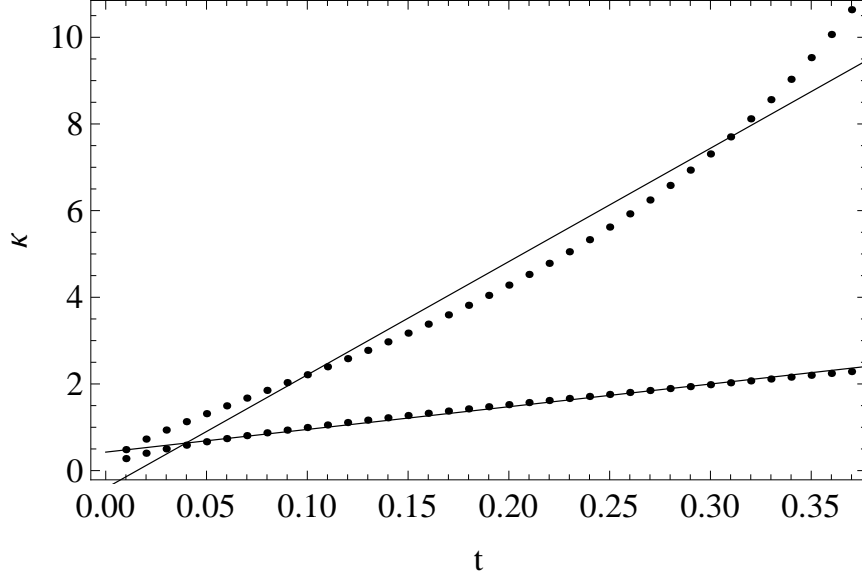


FIG. 10: Parameter space for the pair  $\{t, \kappa\}$ , with fixed  $\lambda_0$  (upper line) and  $\lambda_0/2$  (lower line).

$\lambda = \lambda_0$  and  $\lambda = \lambda_0/2$ , respectively, is shown in Fig. 10; all points in the plot produce the same minimal value for  $Z_M^2$ .

In the case of Fig. 10, a fit with a linear equation produces

$$\kappa = 26.147t - 0.405, \quad (107)$$

with  $\mathcal{R}^2 = 0.991$  for the upper line, and

$$\kappa = 5.239t + 0.426, \quad (108)$$

with  $\mathcal{R}^2 = 0.998$  for the lower line.

## VI. DISCUSSION AND FINAL REMARKS

In the present paper we have provided some preliminary tests at the galactic cluster scale of the hypothesis that dark matter does exist in the form of a Bose-Einstein Condensate. By assuming that the intracluster gas and the dark matter are in hydrostatic equilibrium in the gravitational field created by the total mass of the cluster, and by assuming the knowledge of the hot gas density profile, we have obtained a full description of the observationally relevant properties of BEC dark matter. Then, by using a least- $\chi^2$  fitting between the theoretically derived BEC dark matter mass and the observed cluster mass, by taking into

account the observational data for 106 clusters [21], we have obtained the values of the parameter  $\lambda = m^3/a$  describing the physical properties of the galactic cluster condensate. Astrophysical observations also provide some numerical constraints on the self-interaction cross section of the dark matter. By combining these two sets of information the mass and the scattering length of the dark matter particle can be constrained.

We have investigated first the zero temperature BEC dark matter model, by considering that the dark matter temperature is much lower than the transition one,  $T \ll T_{tr}$ . In this case, the best fitting result is that  $\lambda = (1.766 - 4.755) \times 10^{-96} \text{ g}^3/\text{cm}$ . With the upper limit for self-interaction cross-section,  $\sigma_m \leq 1.25 \text{ cm}^2/\text{g}$ , we derive the upper limits for the dark matter particle mass and scattering length as  $m \leq 1.763 \text{ } \mu\text{eV}$ , and  $a \leq 1.770 \times 10^{-7} \text{ fm}$ , respectively. In the case of the presence of some temperature gradients in the hot intracluster gas, the limits on the mass and scattering length of the dark matter particle, corresponding to  $\lambda = \lambda_1$ , are  $m < 2.5 \times 10^{-3} \text{ meV}$ , and  $a < 2.1 \times 10^{-7} \text{ fm}$ . These bounds are much tighter as compared to the ones obtained from the study of BEC dark matter at the galactic level, which through Eqs. (29) and (30) provides the upper limits  $m \leq 0.179 \text{ meV}$  and  $a \leq 2 \times 10^{-6} \text{ fm}$ , respectively. However, we would like to point out that the galactic estimates are extremely rough, and they are based on qualitative considerations. In order to obtain some better estimates of the mass and scattering length of the dark matter particle from galactic properties, a detailed statistical analysis, also taking into account the effects of the baryonic matter, is required.

The astrophysical parameters of the galactic clusters essentially depend on the cluster central density  $\rho_{DM}(0)$ . In particular,  $\rho_{DM}(0)$  determines the theoretical radius of the cluster, and therefore it can be obtained from the fitting of the theoretical model with the observational data. Hence this property allows the prediction of the cluster mass-central density relation, as well as of the hot gas temperature and cluster central density relation. It is interesting to note that both of these relations can be mathematically described in terms of a simple linear fit, which is statistically significant. Therefore the predicted relations between cluster central density and total mass of the cluster, as well as the predicted relation between gas temperature and  $\rho_{DM}(0)$  may allow a direct astrophysical testing of the BEC dark matter model.

One of the important advances in astronomy in recent years is the observation of large clusters of galaxies, and of the collisions of such clusters. According to the standard  $\Lambda\text{CDM}$

model, when the collision of large clusters takes place, the cosmic gas present in the clusters slows down, and heats up. These processes can be observed through the X-ray radiation emitted by the large amounts of hot ( $10^7$  K) gas located in the collision area. On the other hand, stars and the cold matter halos of galaxies travel through each other without experiencing any collision. Thus cold dark matter halos continue their motion along the initial paths of the colliding clusters, feeling only the effects of the gravitational interactions. Important astrophysical information can be obtained from observations of the weak lensing of the background objects, once they are viewed through the colliding clusters. In this case the deflection angle of the light is proportional to the mass of the gas at the collision point. On the other hand lensing proportional to the sum of the stellar and dark matter masses is seen at the points where visible galaxies are located.

A particularly interesting case is that of the colliding clusters Abell 520 [46]. The lensing observations of the gas-rich core regions of this cluster, containing no visible galaxies, can only be explained by assuming the presence of a dark matter core, which is coincident with the X-ray gas peak, but not with any stellar luminosity peak. These observations are not consistent with the collisionless nature of the cold dark matter in the standard model, and various explanations, like collisional deposition of dark matter, filaments along the line of sight direction, distant background cluster, or distant background cluster, have been proposed [46]. On the other hand, as suggested in [47], if dark matter has a non-zero self-interaction cross-section, as it is the case for Bose-Einstein Condensates, then the dark matter halos of the individual galaxies in the cluster cores must experience a drag force from the ambient dark matter of the cluster. This drag force does not affect the stellar components of galaxies, and consequently this will lead to a separation between the stellar and dark matter components. It was also suggested in [15], that lensing properties of dark matter halos may provide an effective way to distinguish between Bose-Einstein Condensate dark matter and non-interacting dark matter models. The observations of the A520 cluster give an estimate of  $\sigma_m = \sigma/m \approx 3.8 \pm 1.1 \text{ cm}^2 \text{ g}^{-1}$  for the self-interaction cross section of dark matter, a value which must be contrasted with the upper limit  $\sigma_m = \sigma/m < 1.25 \text{ cm}^2/\text{g}$  obtained from the study of the Bullet Cluster [6].

From a thermodynamic point of view a first and fundamental condition that must be satisfied during the cosmological Bose-Einstein Condensation process is the continuity of the dark matter pressure at the transition point. This condition uniquely fixes the critical

transition density  $\rho_{tr}$  from the normal dark matter state to the Bose-Einstein condensed state as [45]

$$\rho_{tr} = 3.868 \times 10^{-21} \left( \frac{\sigma^2}{3 \times 10^{-6}} \right) \times \left( \frac{m}{10^{-33} \text{ g}} \right)^3 \left( \frac{a}{10^{-10} \text{ cm}} \right)^{-1} \text{ g/cm}^3, \quad (109)$$

where  $\sigma^2 = \langle \vec{v}^2 \rangle / 3c^2$ , and  $\langle \vec{v}^2 \rangle$  is the average squared velocity of the bosonic dark matter particle before the BEC phase transition. Therefore from a physical point of view  $\sigma$  can be interpreted as the one-dimensional velocity dispersion.

The critical temperature at the moment of the Bose-Einstein condensation is given by Eq. (1), and it can be obtained as

$$T_{tr} \approx \frac{2\pi\hbar^2}{\zeta(3/2)^{2/3} m^{5/3} k_B} \rho_{tr}^{2/3} = \frac{(2\pi\hbar^2)^{1/3} c^{4/3} (\sigma^2)^{2/3} m^{1/3}}{\zeta(3/2)^{2/3} k_B a^{2/3}}, \quad (110)$$

or, equivalently, in the form

$$T_{tr} \approx 6.57 \times 10^3 \times \left( \frac{m}{10^{-33} \text{ g}} \right)^{1/3} \times \left( \frac{\sigma^2}{3 \times 10^{-6}} \right)^{2/3} \left( \frac{a}{10^{-10} \text{ cm}} \right)^{-2/3} K. \quad (111)$$

By assuming that before the BEC transition the dark matter particles were relativistic, with  $\sigma^2 = 1/3$ , and by considering a dark matter particle mass of the order of  $10^{-39}$  g, with a scattering length of the order of  $10^{-21}$  cm, we obtain a transition density of the order of  $\rho_{tr} \approx 10^{-21}$  g/cm<sup>3</sup>, which is around  $10^8$  times greater than the critical density of the Universe,  $\rho_{cr} \approx 10^{-29}$  g/cm<sup>3</sup>. The corresponding transition temperature is  $T_{tr} \approx 1.41 \times 10^{15}$  K, which is much bigger than the temperature of the intracluster gas, which is of the order of a few keV,  $T_g \approx 10^8$  K. By using these numerical values we can estimate the parameter  $\kappa = m^{1/3} / \rho_{tr}^{1/3} a$  as  $\kappa \approx 10^{15}$ . Hence, taking into account this large value of  $\kappa$ , from Eq. (106) it follows that the finite temperature effects are negligibly small in the case of the BEC dark matter in galactic clusters. However, the finite temperature model for BEC dark matter is a model worth to further explore. Many physical parameters, like the transition density  $\rho_{tr}$  and the transition temperature of dark matter are known only approximately. Moreover, the description of the dark matter properties after the BEC transition certainly needs taking into account finite temperature effects.

An important issue in our study is to try to determine which of the three considered models provides the best fitting of the observational data. Based on the values of  $Z_M^2$  and  $Z_R^2$  in Table I one can make some assessments regarding the model that best fits the observed physical parameters of the considered clusters.

Model	$Z_M^2$	$Z_R^2$	Comments
$T_{BEC} = 0$ , isothermal	2232.63	1249.77	$\lambda = 1.76624$ , $\rho_{DM}(0) = 1.90934$
$T_{BEC} = 0$ , non-isothermal	2273.02	49.5034	$\lambda = 4.20896$ , $\rho_{DM}(0) = 4.10184$
$T_{BEC} \neq 0$ , isothermal	2232.63	-	$\lambda_0 = 1.76624$ and $\{t, \kappa\}$ as in Fig. 10

TABLE I: Values of the test functions  $Z_M^2$  and  $Z_R^2$  for the different models analyzed in this paper.  $\lambda$  is given in units of  $10^{-96} \text{g}^3/\text{cm}$  and  $\rho_{DM}(0)$  in units of  $10^{-13} \text{g}/\text{cm}^3$ .

As one can see from the Table I, the  $Z_M^2$  test function does not change considerably, and there is only a 2% difference between models. However, the value of the  $Z_R^2$  test function is 25 times bigger for the  $T_{BEC} = 0$ , isothermal case than for the non-isothermal case. We consider this as *a statistical evidence that the non-isothermal intracluster hot gas approach should be the preferred paradigm in the analysis of the astrophysical properties of galactic clusters.*

In the present paper we have investigated the properties of the Bose-Einstein condensate dark matter at the galactic cluster scale. But dark matter in its condensate form is also present at the galactic level. In order to obtain a consistent description of the BEC dark matter, the physical properties derived from galaxy and galaxy cluster observations must coincide (in the ideal case), or, due to the uncertainties in the astronomical and astrophysical data, show at least an order of magnitude similarity. The properties of the dark matter particles in the condensate are described by two fundamental parameters, the mass  $m$  and the scattering length  $a$ . From the galactic scale observations the range of  $a$  is given by Eq. (30) as  $a < 2 \times 10^{-6}$  fm, and by Eq. (32) as  $a \in (5 - 27) \times 10^{-8}$  fm. The estimation of  $a$  for the dark matter from galaxy cluster observational data gives, via Eq. (68), the value  $a \approx 2 \times 10^{-7}$  fm. By taking into account the precision of the astronomical data, we may state that these values of  $a$ , obtained from observations at two very different astrophysical scales, indicate at least an order of magnitude agreement with each other. We would also like to point out that the galactic scale values of  $a$  are strongly dependent on the (poorly known) radius of the dark matter halo, for which we have adopted a standard value of  $R = 10$  kpc. Similar correlations can be obtained in the case of the mass of the dark matter particle. The galactic scale values are given by Eqs. (29) and (31) as  $m < 0.2$  meV, and

$m \in (0.05 - 0.09)$  meV, respectively, while the analysis of the 106 galactic clusters provides for the mass of the dark matter particle a value of the order of  $m \approx 1.7 \times 10^{-3}$  meV, given by Eq. (67). The differences in the mass values are much larger than those in the numerical values of the scattering lengths. It is matter of further study to find out if these differences are due to the uncertainties in the astronomical/astrophysical data, to the limitations of the used theoretical models, to the statistical methods used in data analysis, or if they show an intrinsic conflict between the BEC dark matter models at the galactic and extragalactic scales.

### Acknowledgement

We would like to thank to the anonymous referee for comments and suggestions that helped us to improve our manuscript. S.-D. L. gratefully acknowledges financial support for this project from the Fundamental Research Fund of China for the Central Universities. GM is partially supported by a grant of the Romanian National Authority of Scientific Research, Program for research - Space Technology and Advanced Research - STAR, project number 72/29.11.2013.

- 
- [1] J. M. Overduin and P. S. Wesson, *Physics Reports* **402**, 267 (2004).
  - [2] H. Baer, K.-Y. Choi, J. E. Kim, and L. Roszkowski, *Physics Reports* **555**, 1 (2015).
  - [3] D. V. Ahluwalia-Khalilova and D. Grumiller, *Phys. Rev. D* **72**, 067701 (2005); C. Destri, H. J. de Vega, and N. G. Sanchez, *New Astronomy* **22**, 39 (2013); G. Grams, R. C. de Souza, and G. M. Kremer, *Class. Quantum Grav.* **31**, 185008 (2014).
  - [4] B. Fuchs and E. W. Mielke, *Mon. Not. Roy. Astron. Soc.* **350**, 707 (2004); F. E. Schunck, B. Fuchs, and E. W. Mielke, *Mon. Not. Roy. Astron. Soc.* **369**, 485 (2006); A. Bernal and F. Siddhartha Guzman, *Phys. Rev. D* **74**, 103002 (2006); B. Li and J. D. Barrow, *Phys. Rev. D* **83**, 024007 (2011).
  - [5] T. Harko and K. S. Cheng, *Phys. Rev. D* **76**, 044013 (2007); O. Bertolami, C. G. Boehmer, T. Harko, and F. S. N. Lobo, *Phys. Rev. D* **75**, 104016 (2007); C. G. Boehmer, T. Harko, and F. S. N. Lobo, *JCAP* **0803**, 024 (2008); H. R. Sepangi and S. Shahidi, *Class. Quant. Grav.*

- 26**, 185010 (2009); A. S. Sefiedgar, K. Atazadeh, and H. R. Sepangi, Phys. Rev. **D 80**, 064010 (2009); A. S. Sefiedgar, Z. Haghani, and H. R. Sepangi, Phys. Rev. **D 85**, 064012 (2012); O. Bertolami, P. Frazao, and J. Paramos, Phys. Rev. **D 86**, 044034 (2012); L. Lombriser, F. Schmidt, T. Baldauf, R. Mandelbaum, U. Seljak, and R. E. Smith, Phys. Rev. **D 85**, 102001 (2012); S. Capozziello, T. Harko, T. S. Koivisto, F. S. N. Lobo, and G. J. Olmo, JCAP **07** (2013) 024; T. Harko, F. S. N. Lobo, M. K. Mak, and S. V. Sushkov, Mod. Phys. Lett. **A 29**, 1450049 (2014).
- [6] D. Harvey, R. Massey, T. Kitching, A. Taylor, and E. Tittley, Science **347**, 1462 (2015).
- [7] E. D. Carlson, M. E. Machacek, and J. L. Hall, Astrophys. J. **398**, 43 (1992); A. A. de Laix, R. J. Scherrer, and R. K. Schaefer, Astrophys. J. **452**, 495 (1995); C. J. Saxton and I. Ferreras, Monthly Notices of the Royal Astronomical Society **405**, 77 (2010); C. J. Saxton, Monthly Notices of the Royal Astronomical Society **430**, 1578 (2013).
- [8] M. Vogelsberger, J. Zavala, and A. Loeb, Monthly Notices of the Royal Astronomical Society **423**, 3740 (2012).
- [9] A. Robertson, R. Massey, V. Eke, and R. Bower, arXiv:1505.02046 (2015).
- [10] S. N. Bose, Z. Phys. **26**, 178 (1924).
- [11] A. Einstein, Sitzungsberichte der Preussischen Akademie der Wissenschaften, Physikalisch-mathematische Klasse, **1924**, 261 (1924); A. Einstein, Sitzungsberichte der Preussischen Akademie der Wissenschaften, Physikalisch-mathematische Klasse, **1925**, 3 (1925).
- [12] M. H. Anderson, J. R. Ensher, M. R. Matthews, C. E. Wieman, and E. A. Cornell, Science **269**, 198 (1995); C. C. Bradley, C. A. Sackett, J. J. Tollett, and R. G. Hulet, Phys. Rev. Lett. **75**, 1687 (1995); K. B. Davis, M. O. Mewes, M. R. Andrews, N. J. van Druten, D. S. Durfee, D. M. Kurn, and W. Ketterle, Phys. Rev. Lett. **75**, 3969 (1995).
- [13] P. H. Chavanis and T. Harko, Phys. Rev. **D 86**, 064011 (2012); X. Y. Li, T. Harko, and K. S. Cheng, JCAP **06**,001 (2012); X. Y. Li, F. Wang, and K. S. Cheng, JCAP **10**, 031 (2012); P. H. Chavanis, arXiv:1412.0005 (2014); S. Latifah, A. Sulaksono, and T. Mart, Phys. Rev. **D 90**, 127501 (2014); A. Mukherjee, S. Shah, and S. Bose, Phys. Rev. **D 91**, 084051 (2015); B. Danila, T. Harko, and Z. Kovacs, Eur. Phys. J. **C 75**, 203 (2015).
- [14] M. Membrado, A. F. Pacheco, and J. S. Sanudo, Astron. Astrophys. **217**, 92 (1989); J. Sin, Phys. Rev. **D 50**, 3650 (1994); S. U. Ji and S. J. Sin, Phys. Rev. **D50**, 3655 (1994); M. Membrado and J. A. L. Aguerra, Int. J. Mod. Phys. **D 5**, 257 (1996); M. Membrado,

- Monthly Notices of the Royal Astronomical Society **296**, 21 (1998); W. Hu, R. Barkana, and A. Gruzinov, Phys. Rev. Lett. **85** 1158, (2000); J. Goodman, New Astronomy **5**, 103 (2000); P. J. E. Peebles, Astrophys. J. **534**, L127 (2000); A. Arbey, J. Lesgourgues and P. Salati, Phys. Rev. **D 68**, 023511 (2003).
- [15] C. G. Boehmer and T. Harko, JCAP **06**, 025 (2007).
- [16] J.-W.Lee, Phys. Lett. **B 681**, 118 (2009); J.-W. Lee and S. Lim, JCAP **1001**, 007 (2010); V. H. Robles and T. Matos, Mon. Not. Roy. Astron. Soc. **422**, 282 (2012); M. Dwornik, Z. Keresztes, and L. A. Gergely, Chapter 6 of “Recent Development in Dark Matter Research”, Eds. N. Kinjo, A. Nakajima, Nova Science Publishers (2014), arXiv:1312.3715; F. S. Guzman, F. D. Lora-Clavijo, J. J. Gonzalez-Aviles, and F. J. Rivera-Paleo, arXiv:1310.3909 (2013); T. Harko and E. J. M. Madarassy, JCAP **01**, 020 (2012); B. Kain and H. Y. Ling, Phys. Rev. **D 82**, 064042 (2010); N. T. Zinner, Physics Research International **2011**, 734543 (2011); P.-H. Chavanis, Phys. Rev. **D 84**, 043531 (2011); P.-H. Chavanis and L. Delfini, Phys. Rev. **D 84**, 043532 (2011); P.-H. Chavanis, Phys. Rev. **D 84**, 063518 (2011); P.-H. Chavanis, Phys. Rev. **E 84**, 031101 (2011); T. Rindler-Daller and P. R. Shapiro, Mon. Not. Roy. Astron. Soc. **422**, 135 (2012); T. Rindler-Daller and P. R. Shapiro, arXiv:1312.1734 (2013); M. O. C. Pires and J. C. C. de Souza, JCAP **11**, 024 (2012); T. Harko, Mon. Not. Roy. Astron. Soc. **413**, 3095 (2011); P.-H. Chavanis, Astron. Astrophys. **537**, A127 (2012); R. C. Freitas and S. V. B. Goncalves, JCAP **04**, 049 (2013); H. Velten and E. Wamba, Phys. Lett. **B 709**, 1 (2012); E. J. M. Madarassy and V. T. Toth, Computer Physics Communications **184**, 1339 (2013); F. S. Guzman, F. D. Lora-Clavijo, J. J. Gonzalez-Aviles, and F. J. Rivera-Paleo, JCAP **09**, 034 (2013); J. C. C. de Souza and M. O. C. Pires, arXiv:1401.6142 (2014); V. T. Toth, arXiv:1402.0600 (2014); T. Harko, Phys. Rev. **D 89**, 084040 (2014); M.-H. Li and Z.-B. Li, Phys. Rev. **D 89**, 103512 (2014); T. Harko and M. J. Lake, Phys. Rev. **D 91**, 045012 (2015); E. J. M. Madarassy and V. T. Toth, Phys. Rev. **D 91**, 044041 (2015); J. C. C. de Souza and M. Ujevic, Gen. Rel. Grav. **47**, 100 (2015); T. Harko and F. S. N. Lobo, Phys. Rev. **D 92**, 043011 (2015); H.-Y. Schive, T. Chiueh, T. Broadhurst, and K.-W. Huang, arXiv:1508.04621 (2015).
- [17] T. Harko, JCAP **1105**, 022 (2011).
- [18] T. Harko and G. Mocanu, Phys. Rev. **D 85**, 084012 (2012).
- [19] J. Binney and S. Tremaine S, Galactic dynamics, Princeton, N. J.; Woodstock: Princeton



University Press (2008)

- [20] A. V. Kravtsov and S. Borgani, *Annual Review of Astronomy and Astrophysics* **50**, 353 (2012).
- [21] T. H. Reiprich and H. Boehringer, *Astrophys. J.* **567**, 716 (2002).
- [22] J. C., Nash, *Compact Numerical Methods for Computers: Linear Algebra and Function Minimization*, 2nd ed. Bristol, England: Adam Hilger, 1990.
- [23] A. Griffin, T. Nikuni, and E. Zaremba, *Bose-condensed gases at finite temperatures*, Cambridge, Cambridge University Press, (2009).
- [24] T. Harko and E. J. M. Madarassy, *JCAP* **01**, 020 (2011).
- [25] E. Zaremba, T. Nikuni, and A. Griffin, *Journal of Low Temperature Physics*, **116**, 277 (1999).
- [26] N. P. Proukakis and B. Jackson, *J. Phys. B: At. Mol. Opt. Phys.* **41**, 203002 (2008).
- [27] Yu. Kagan and B. V. Svistunov, *Phys. Rev. Lett.* **79**, 3331 (1997); D. A. W. Hutchinson, E. Zaremba, and A. Griffin, *Phys. Rev. Lett.* **78**, 1842 (1997); M. J. Davis, S. A. Morgan, and K. Burnett, *Phys. Rev. A* **66**, 053618 (2002).
- [28] A. Griffin, *Phys. Rev. B* **53**, 9341 (1996); S. Giorgini, *Phys. Rev. A* **57**, 2949 (1998); M. Imamović-Tomasović and A. Griffin, *Phys. Rev. A* **60**, 494 (1999).
- [29] J. E. Robinson, *Phys. Rev.* **83**, 678 (1951).
- [30] S. W. Randall, M. Markevitch, D. Clowe, A. H. Gonzalez, and M. Bradac, *Astrophys. J.* **679**, 1173 (2008).
- [31] R. Massey, T. Kitching, and D. Nagai, *Monthly Notices of the Royal Astronomical Society* **413**, 1709 (2011).
- [32] M. Arnaud, X-ray observations of clusters of galaxies, in *Background Microwave Radiation and Intracluster Cosmology*, Proceedings of the International School of Physics Enrico Fermi, Edited by F. Melchiorri and Y. Rephaeli, Published by IOS Press, The Netherlands, and Societa Italiana di Fisica, Bologna, Italy, p. 77, (2005).
- [33] P. Schuecker, H. Böhringer, K. Arzner and T. H. Reiprich, *Astron. Astrophys.* **370**, 715 (2001); M. Baldi, V. Pettorino, G. Robbers, and V. Springel, *Mon. Not. R. Astron. Soc.* **403**, 1684 (2010); B. Li and J. D. Barrow, *Phys. Rev. D* **83**, 024007 (2011).
- [34] D. Ejlli, *Phys. Rev. D* **90**, 123527 (2014).
- [35] C. Beck, *Phys. Rev. Lett.* **111**, 231801 (2013).
- [36] M. Markevitch, W. R. Forman, C. L. Sarazin, and A. Vikhlinin, *Astrophys. J.* **503**, 77 (1998).
- [37] C. Loken, M. L. Norman, E. Nelson, J. Burns, G. L. Bryan, and P. Motl, *Astrophys. J.* **579**,

- 571 (2002).
- [38] L. Lovisari, T. Reiprich, and G. Schellenberger, *Astron. Astrophys.* **573**, A118 (2015).
  - [39] A. Vikhlinin, M. Markevitch, S. S. Murray, C. Jones, W. Forman, and L. Van Speybroeck, *Astrophys. J.* **628**, 655 (2005).
  - [40] A. E. Evrard, C. A. Metzler, and J. F. Navarro, *Astrophys. J.* **469**, 494 (1996).
  - [41] F. Durret, G. B. Lima Neto, and W. Forman, *Astron. Astrophys.* **432**, 809 (2005).
  - [42] F. Gastaldello, D. A. Buote, P. J. Humphrey, L. Zappacosta, J. S. Bullock, F. Brighenti, and W. G. Mathews, 2007, *Astrophys. J.* **669**, 158 (2007).
  - [43] Y. Sofue, M. Honma, and T. Omodaka, *Publications of the Astronomical Society of Japan* **61**, 227 (2009).
  - [44] M. H. Chan and M. C. Chu, *Astrophys. Space Sci.* **317**, 149 (2008).
  - [45] T. Harko, *Phys. Rev. D* **83**, 123515 (2011).
  - [46] M. J. Jee, A. Mahdavi, H. Hoekstra, A. Babul, J. J. Dalcanton, P. Carroll, and P. Capak, *ApJ* **747**, 96 (2012).
  - [47] L. L. R. Williams and P. Saha, *Monthly Notices of the Royal Astronomical Society* **415**, 448 (2011).